SMC-TR-01-05

AEROSPACE REPORT NO.
TR-2000(1490)-3

Puff Dispersion Sigma Values from MVP4 at VAFB

June 29, 2000

Prepared by

I. A. MIN
Space Architecture Department
Systems Engineering Division
Engineering and Technology Group

Prepared for

SPACE AND MISSILE SYSTEMS CENTER
AIR FORCE MATERIEL COMMAND
2430 E. El Segundo Boulevard
Los Angeles Air Force Base, CA 90245

Contract No. F04701-93-C-0094

Space Systems Group

APPROVED FOR PUBLIC RELEASE; DISTRIBUTION UNLIMITED.

THE AEROSPACE CORPORATION
El Segundo, California

20010305 109

This report was submitted by The Aerospace Corporation, El Segundo, CA 90245-4691, under Contract No. F04701-93-C-0094 with the Space and Missile Systems Center, Air Force Materiel Command, 2430 E. El Segundo Blvd., Los Angeles Air Force Base, CA 90245. It was reviewed and approved for The Aerospace Corporation by Dr. P. L. Smith, Principal Director, Architecture & Design Subdivision. The project officer is 2nd Lieutenant Michael Keough.

This report has been reviewed by the Public Affairs Office (PAS) and is releasable to the National Technical Information Service (NTIS). At NTIS, it will be available to the general public, including foreign nations.

This technical report has been reviewed and is approved for publication. Publication of this report does not constitute Air Force approval of the report's findings or conclusions. It is published only for the exchange and stimulation of ideas.

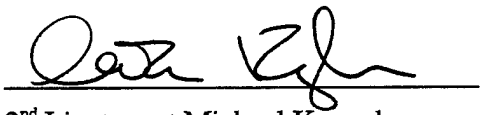

2nd Lieutenant Michael Keough
Project Officer

REPORT DOCUMENTATION PAGE

Form Approved
OMB No. 0704-0188

Public reporting burden for this collection of information is estimated to average 1 hour per response, including the time for reviewing instructions, searching existing data sources, gathering and maintaining the data needed, and completing and reviewing the collection of information. Send comments regarding this burden estimate or any other aspect of this collection of information, including suggestions for reducing this burden, to Washington Headquarters Services, Directorate for Information Operations and Reports, 1215 Jefferson Davis Highway, Suite 1204, Arlington, VA 22202-4302, and to the Office of Management and Budget, Paperwork Reduction Project (0704-0188), Washington, DC 20503.

1. AGENCY USE ONLY (Leave blank)	2. REPORT DATE	3. REPORT TYPE AND DATES COVERED
	June 29, 2000	

4. TITLE AND SUBTITLE

Puff Dispersion Sigma Values from MVP4 at VAFB

5. FUNDING NUMBERS

6. AUTHOR(S)

Inki A. Min

7. PERFORMING ORGANIZATION NAME(S) AND ADDRESS(ES)

The Aerospace Corporation
2350 E. El Segundo Blvd
El Segundo, CA 90245-4691

8. PERFORMING ORGANIZATION REPORT NUMBER

TR-2000(1490)-3

9. SPONSORING/MONITORING AGENCY NAME(S) AND ADDRESS(ES)

Space and Missile Systems Center
Air Force Materiel Command
2350 E. El Segundo Blvd
Los Angeles Air Force Base, CA 90245

10. SPONSORING/MONITORING AGENCY REPORT NUMBER

SMC-TR-01-05

11. SUPPLEMENTARY NOTES

12a. DISTRIBUTION/AVAILABILITY STATEMENT

Approved for public release; distribution unlimited.

12b. DISTRIBUTION CODE

13. ABSTRACT (Maximum 200 words)

This report documents the calculation of σ values (standard deviation of material distribution) for several series of SF_6 puffs released over Vandenberg Air Force Base (VAFB) in May 1997 as part of the Model Validation Program (MVP). Using an assumption of Gaussianity for the distribution of the material, the σ values are calculated based on measurements of maximum visual extent of the puffs provided by R. Abernathy[1]. Turbulence fluctuation values derived from the σ values can be used for the evaluation of REEDM's turbulence algorithm.

14. SUBJECT TERMS

15. NUMBER OF PAGES
49

16. PRICE CODE

17. SECURITY CLASSIFICATION OF REPORT	18. SECURITY CLASSIFICATION OF THIS PAGE	19. SECURITY CLASSIFICATION OF ABSTRACT	20. LIMITATION OF ABSTRACT
Unclassified	Unclassified	Unclassified	Unlimited

[1]R. N. Abernathy, "MVP Deployment 4 (May 1977) – Tracer Gas Atmospheric Dispersion Measurements at Vandenberg Air Force Base," TR, 2000.

Acknowledgements

The analysis performed in this report is based on the experimental data obtained from the Model Validation Program (MVP), managed by Dr. H. L. Lundblad of Environmental Systems. The puff imagery was collected by the MVP team, including members of the Surveillance Technologies Department of The Aerospace Corporation. The imagery analysis performed by Dr. R. N. Abernathy, who provided the puff data and shared many insights related to the data collection, was essential to the preparation of this report. The assistance of T. Barros in preparation of the figures is also appreciated.

Puff Dispersion Sigma Values from MVP4 at VAFB

I. A. Min

29 June 2000

Abstract

This report documents the calculation of σ values (standard deviations of material distribution) for several series of SF_6 puffs released over Vandenberg Air Force Base (VAFB) in May of 1997 as part of the Model Validation Program (MVP). Assuming a Gaussian distribution, estimates of the σ values are calculated based on measurements of maximum visual extent of the puffs provided by R. Abernathy [1]. Turbulence fluctuation values derived from the σ values can be used for the evaluation of REEDM's turbulence algorithm.

1 Introduction

Turbulent dispersion at launch sites are of interest because it is the mechanism by which the toxic material in the launch exhaust clouds left behind during rocket launches are spread. The purpose of the present investigation is to validate the turbulence model in the Rocket Exhaust Effluent Dispersion Model (REEDM), which is used operationally to support launches in the Eastern Range (Cape Canaveral Air Force Station) and the Western Range (Vandenberg Air Force Base). This validation effort is one of the goals of the Model Validation Program (MVP).

On the 21st and the 23rd of May 1997, several series of SF_6 puffs were released from a blimp located near SLC-4, at an altitude of about 1000 m. The boundary layer height was about 400 m on those days, so the puff imagery gives information about turbulence above the boundary layer. The typical vertical extent of the launch cloud after stabilization is between 400 to 1200 m at Vandenberg, so the puffs were probing dispersion within the envelope of interest.

The raw imagery data from three or four simultaneous infrared cameras was processed and compiled by R. Abernathy [1] into estimates of the maximum along-wind and cross-wind puff dimensions. Also provided were the dimensions perpendicular to each of the along and cross-wind dimensions, in the image. This information is used to derive the standard deviations of the material distribution in the puff (σ_x and σ_y). The rates of increase of σ_x and σ_y are used to estimate the turbulence intensities ($i = \sigma_u/U$ or σ_v/U).

The descriptions of the experiments and data acquisition are detailed in reference [1] and are not discussed here. In section 2, a brief account of the methodology used to calculate σ from the visual extent of the puffs is given. The σ data is presented in section 3 in graphical format while section 4 summarizes the data.

2 Data Analysis Methodology

The quantities measured by the infrared cameras are the maximum along and cross-wind dimensions of the puffs at various times during their dispersion. Also recorded are the dimensions perpendicular to each maximum dimension. The quantities of interest in dispersion modeling are the standard deviations of the concentration distribution in the along and cross-wind directions (σ_x and σ_y). The vertical concentration distribution (σ_z) could not be ascertained with sufficient confidence for these experiments because of the camera angles.

Traditionally, estimates of the standard deviations of the material distribution in a puff are based [10, 8, 6, 4, 7] on photographic images of the line-integrated puff material (usually smoke particles). Assuming that the distribution of the material in a puff is Gaussian, the value of the integrated (column) density at the visible outline is estimated by the use of the maximum length (or width) attained by image over time. Högström [5] extends this technique to allow the observation of both the length and height of the puff.

The technique described in this report improves upon the traditional approach in two ways. The first is the use of multiple cameras (2, 3, or 4) to get simultaneous images of the puffs from different angles. (Frenkiel and Katz [3] also used two cameras.) Simultaneous pairwise images are considered and filtered for acceptability for consideration as along or cross-wind view. This technique allows for improved determination of the puff location, as well as puff orientation.

The second improvement is the use of infrared cameras to image the SF_6 puffs, which allows the use of the pixel intensity information to calculate the actual value of the the line-integrated concentration (column density) of the SF_6, as formulated by Polak and Knudtson [9]. This technique eliminates the need to peg the estimation of the line-integrated material density to the maximum radius achieved by the cloud.

Figures 1 and 2 show the distribution of the column density or line-of-sight integrated concentration values for a puff image (Series 3, Puff 1, May 21). The column density is related to the pixel brightness in the infrared image, which was processed and provided by Abernathy [2]. A relatively sharp delineation of the puff boundary can be seen in these figures, imposed by the noise in the image at a column density of about 1 ppm-m. Figures 3 and 4 show similar surface and contour plots for a different image (Series 1, PUff 1, May 21). A smoothing algorithm was applied to these figures for improved visibility.

Assuming a Gaussian distribution of the material (in all three directions), and assuming an elliptical shape (so that when $y = D_A/2$, $z = 0$ on the Γ_0 = constant contour), the equation for Γ_0,

$$\Gamma_0 = \frac{Q}{2\pi\sigma_A^2 D_{perp}/D_A} e^{-(D_A/2)^2/2\sigma_A^2} \tag{1}$$

where Q is the mass of SF_6 in the puff, D_A, D_C, and D_{perp} are the maximum along-wind, cross-wind, and perperdicular visible extent of the puff, respectively. Γ_0 is the column density at the maximum visible extent of the puff. Eq (1) can be solved using Newton-Raphson method for σ_A. A solution for σ_C is obtained similarly using

$$\Gamma_0 = \frac{Q}{2\pi\sigma_C^2 D_{perp}/D_C} e^{-(D_C/2)^2/2\sigma_C^2}. \tag{2}$$

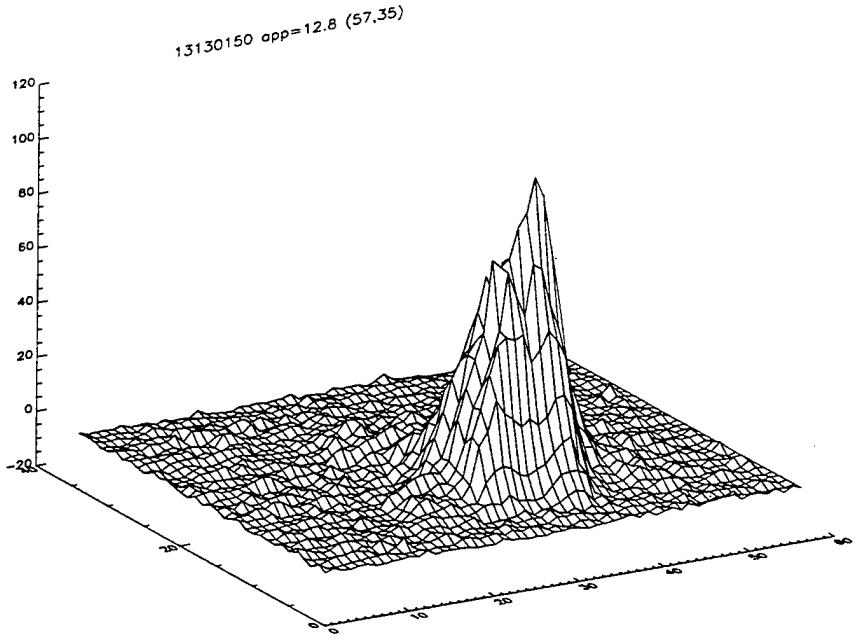

Figure 1: Column density ($ppm - m$) versus along-wind and vertical dimensions (m x m) for May 21, Series 3 Puff 1 image from camera 3 at t=150 s

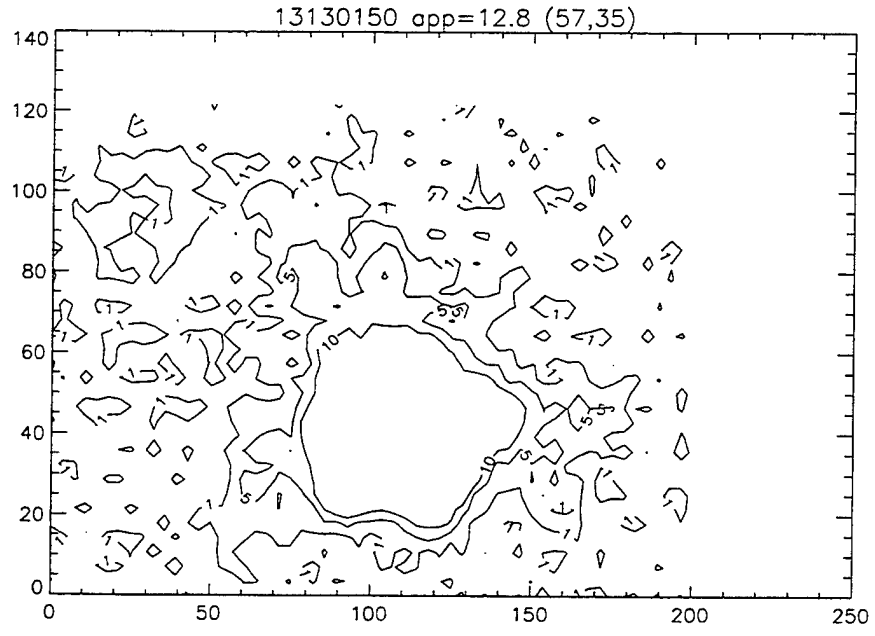

Figure 2: Column density ($ppm - m$) versus along-wind and vertical dimension (m x m) for May 21, Series 3 Puff 1 image from camera 3 at t=150 s

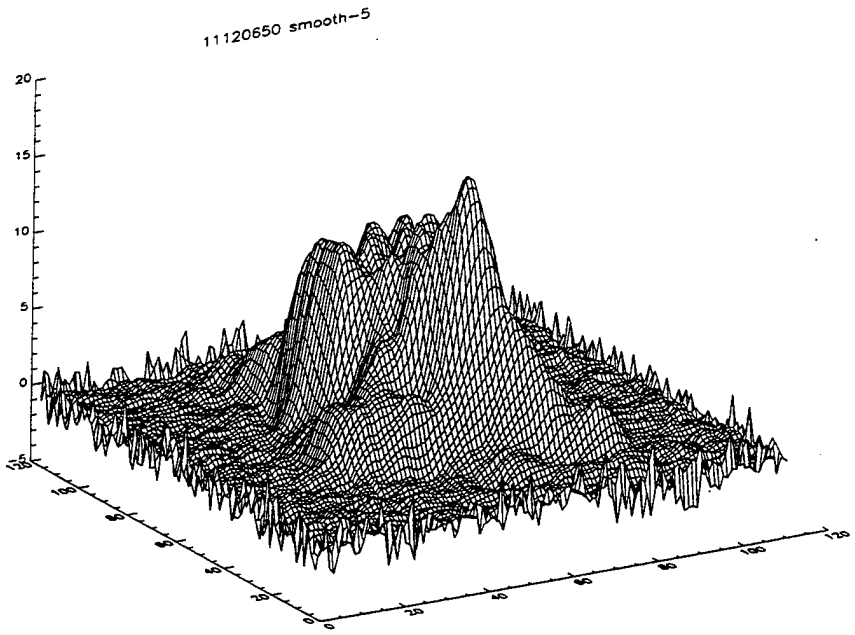

Figure 3: Column density ($ppm - m$) versus cross-wind and vertical dimensions (m x m) for May 21, Series 1 Puff 1 image from camera 2 at t=650 s

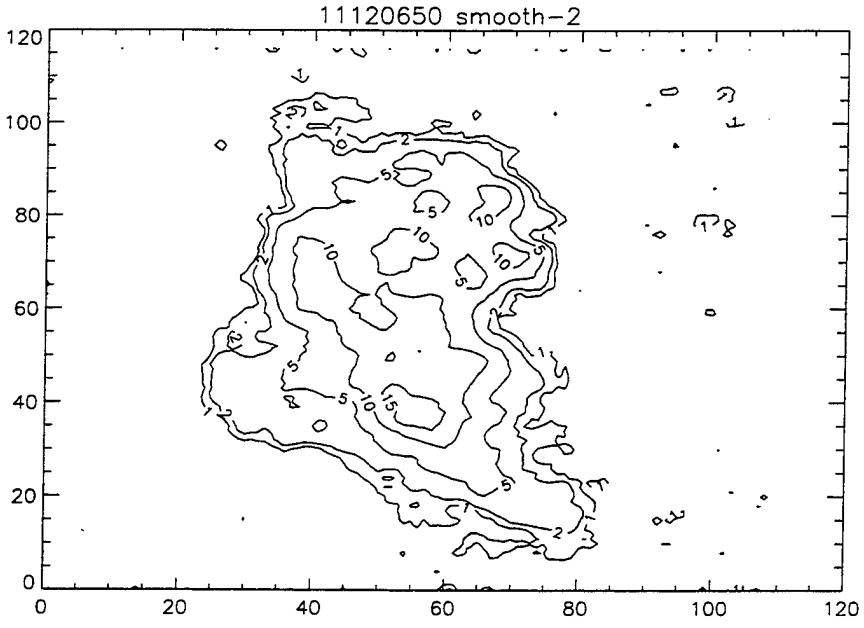

Figure 4: Column density ($ppm - m$) versus cross-wind and vertical dimension (m x m) for May 21, Series 1 Puff 1 image from camera 2 at t=650 s

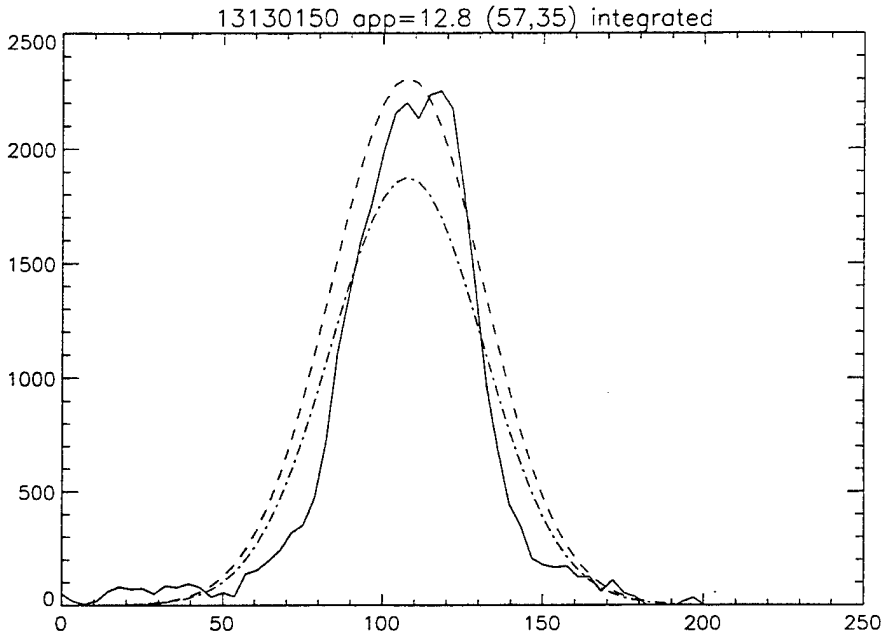

Figure 5: Integrated column density ($ppm-m^2$) versus along-wind (m) for May 21, Series 3 Puff 1 image from camera 3 at t=150 s

Γ_0 is estimated to have a value of about 1 ppm-m from examination of the processed infrared images. There is actually significant variation in the exact value of Γ_0, ranging from less than 0.5 to greater than 2, due to the continually varying line-of-sight and relative position with respect to neighboring puffs. The calculated σ is somewhat sensitive to the value of Γ_0 assumed, but 1 ppm-m is a reasonable compromise that bounds the possible error to less than $\pm 30\%$.

Figure 5 shows the result when the the column density values are integrated along the vertical direction. The profile is compared against Gaussian curves for two different assumptions of the mass contained in the puff using 1) $Q = M_A$(average puff SF_6 mass) and 2) $Q = M_I$(imagery-derived mass). It can be seen that the Gaussian assumption is reasonable. The Gaussian assumption is best applied for ensemble averages and is less valid for single realizations. Figure 6 shows a similar plot for a different image.

Ideally, σ_C and σ_A should be calculated by direct integration of the column densities derived from the pixel intensities. It is not feasible to do the detailed analysis of each image required for the direct integration; however, it was done for several images to validate the approximate Gaussian approach. Figures 7 and 8 show comparisons of data from the two techniques for Series 1 Puff 1 and Series 2 Puff 1, both from May 21. The figures show that there is reasonable agreeement in the estimate of σ. Specific discrepancies can be attributed to several possible sources, including the estimate of Γ_0 at the edge, the loss of mass outside the detectable edge, and the Gaussian assumption. Abernathy [1] has observed that although there are significant variations from puff to puff, the extent of the puff derived from the imagery included the bulk of the SF_6 tracer.

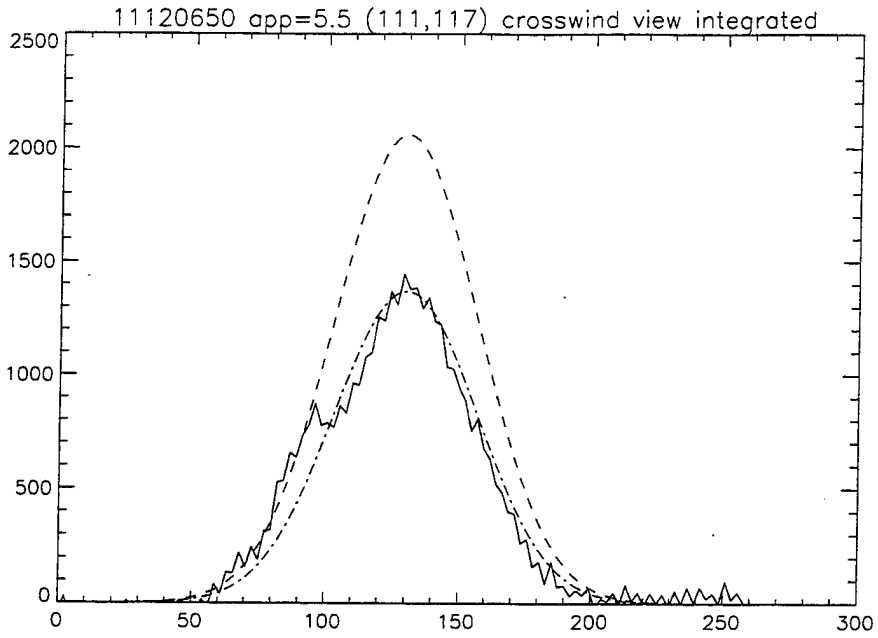

Figure 6: Integrated column density ($ppm - m^2$) versus cross-wind (m) for May 21, Series 1 Puff 1 image from camera 2 at t=650 s

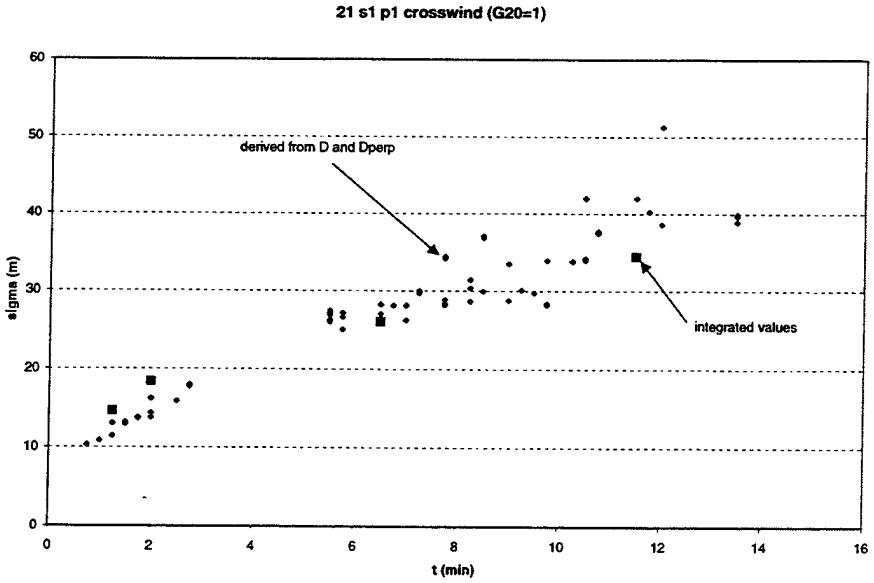

Figure 7: Comparison of cross-wind σ_C derived from direct integration and Gaussian assumption, Series 1 Puff 1, May 21

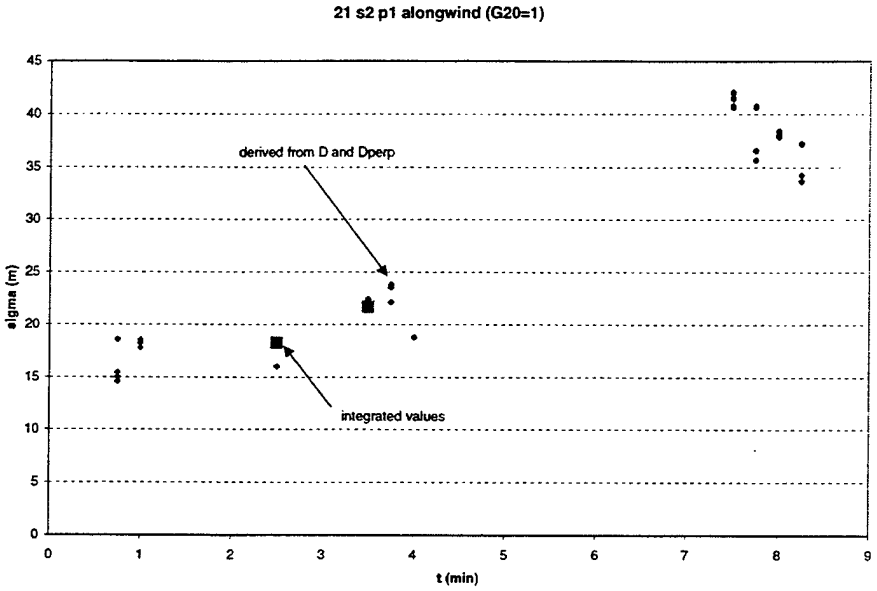

Figure 8: Comparison of along-wind σ_A derived from direct integration and Gaussian assumption, Series 2 Puff 1, May 21

3 Sigma Data

The estimates of σ_A and σ_C are presented graphically in this section. The time histories of σ development for 27 puffs (including along and cross-wind profiles) are shown for May 21 in Figures 10 through 35. For May 23, 46 puff σ estimates are shown in Figures 38 through 81.

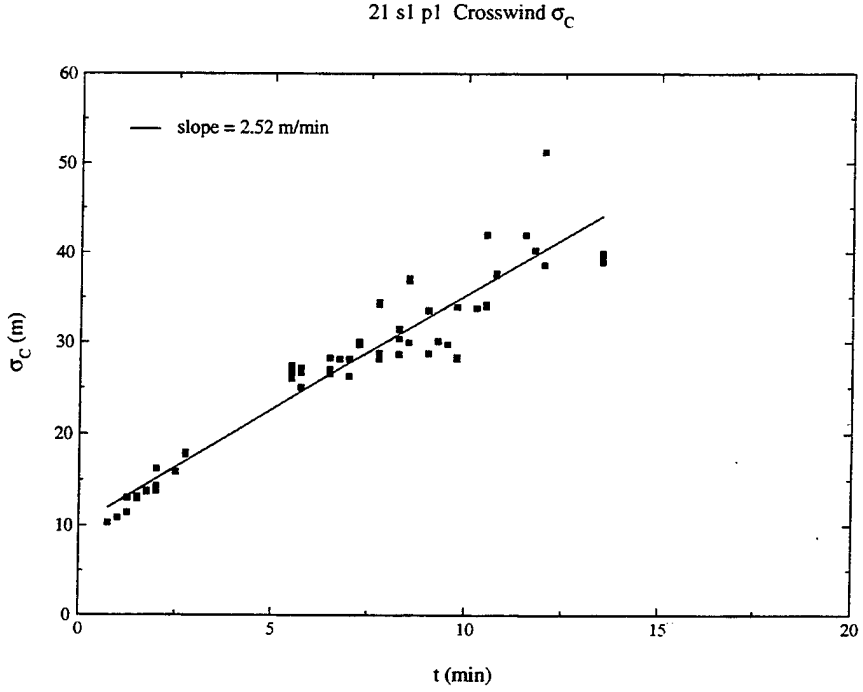

Figure 9: May 21 series 1 puff 1 Crosswind σ

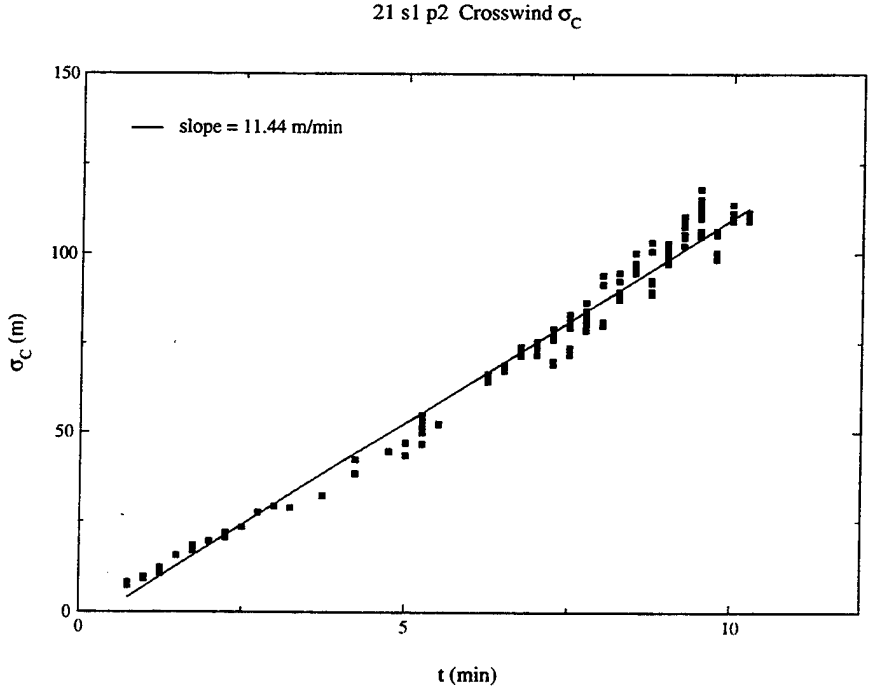

Figure 10: May 21 series 1 puff 2 Crosswind σ

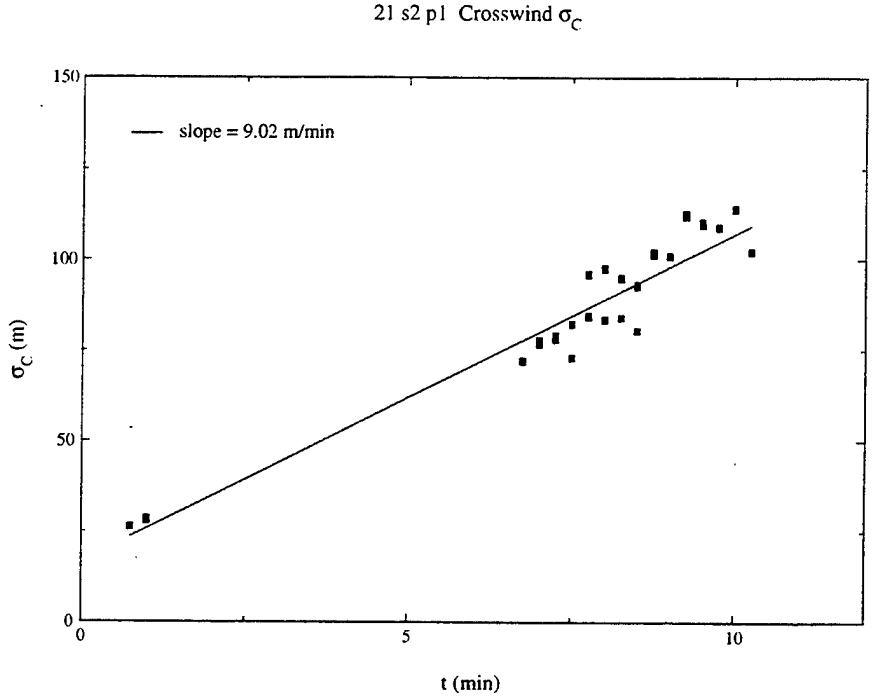

Figure 11: May 21 series 2 puff 1 Crosswind σ

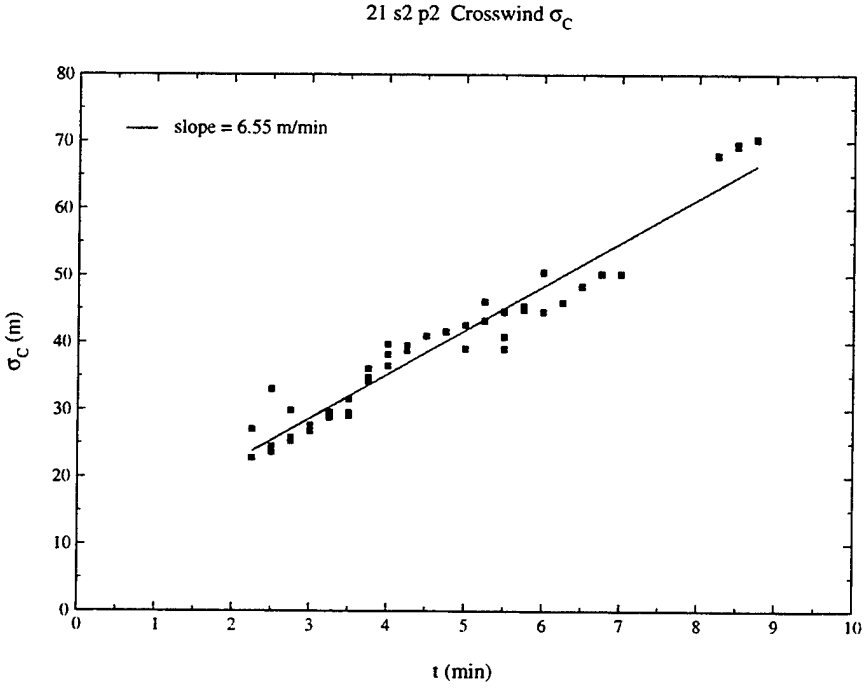

Figure 12: May 21 series 2 puff 2 Crosswind σ

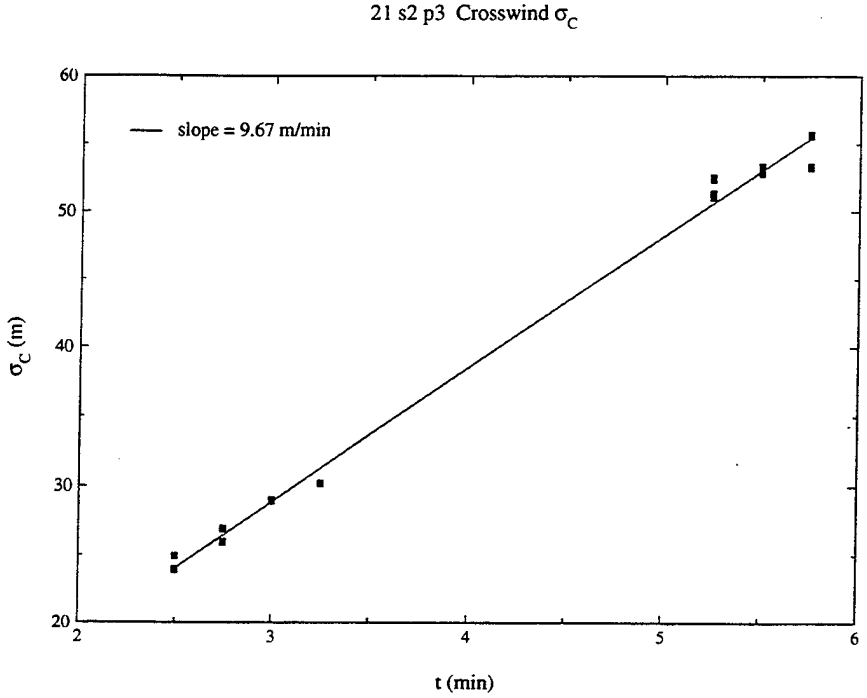

Figure 13: May 21 series 2 puff 3 Crosswind σ

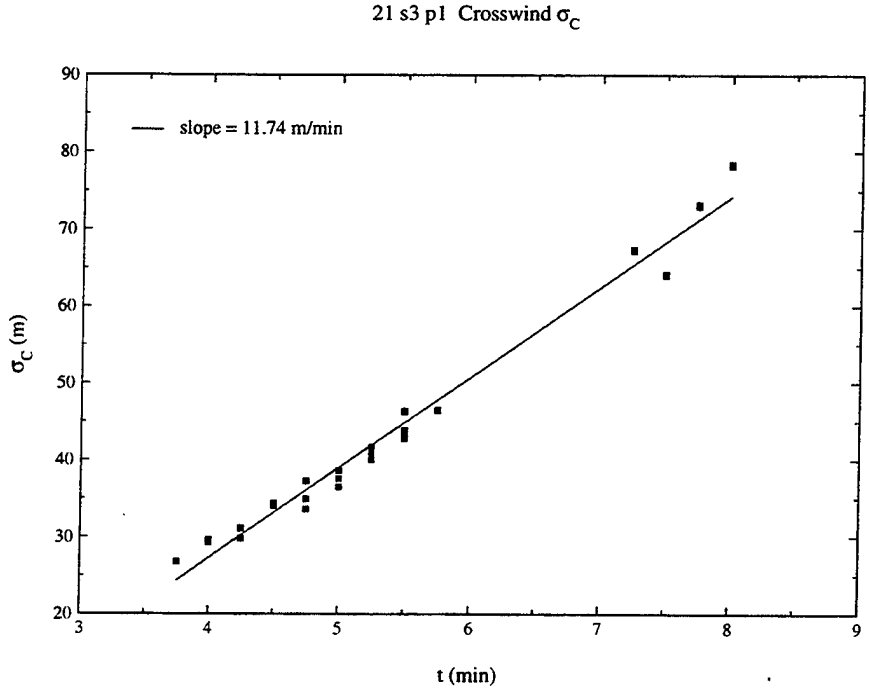

Figure 14: May 21 series 3 puff 1 Crosswind σ

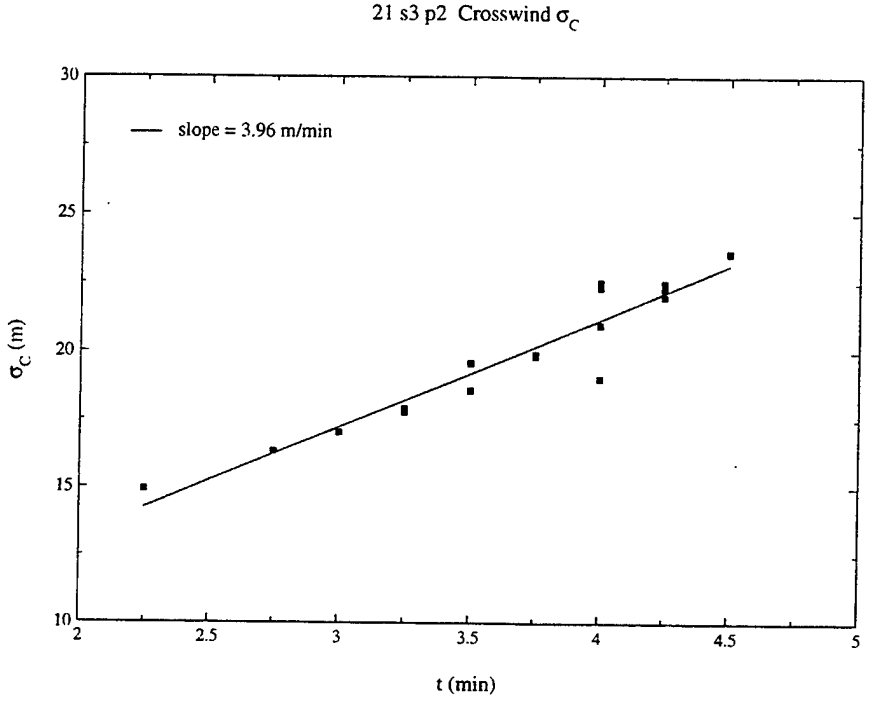

Figure 15: May 21 series 3 puff 2 Crosswind σ

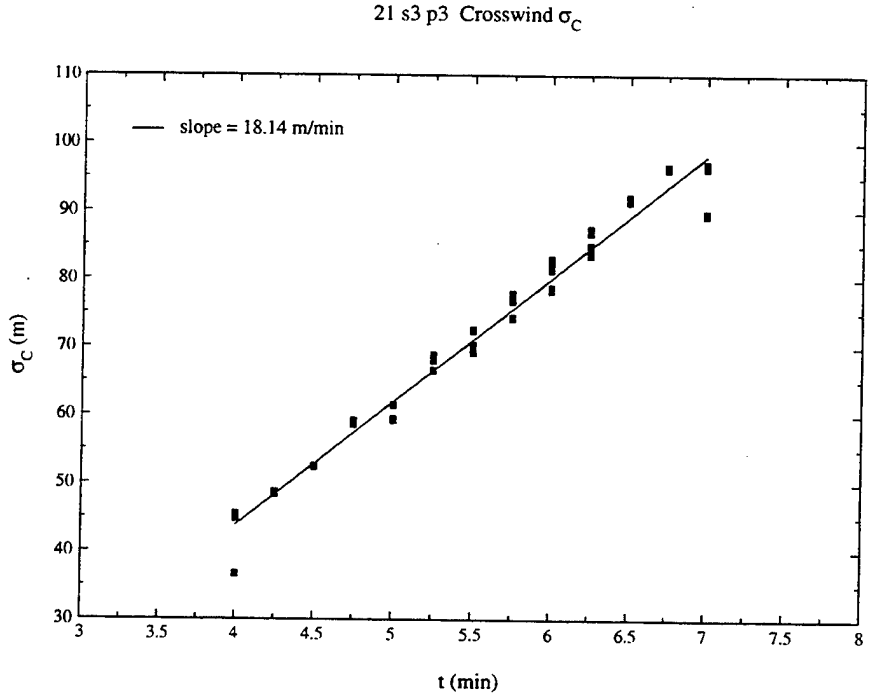

Figure 16: May 21 series 3 puff 3 Crosswind σ

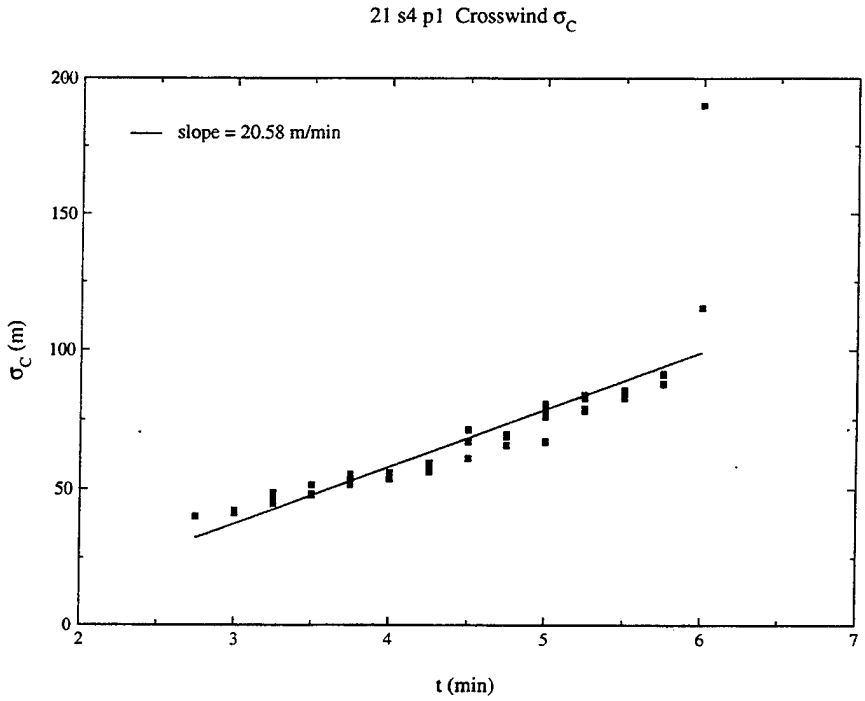

Figure 17: May 21 series 4 puff 1 Crosswind σ

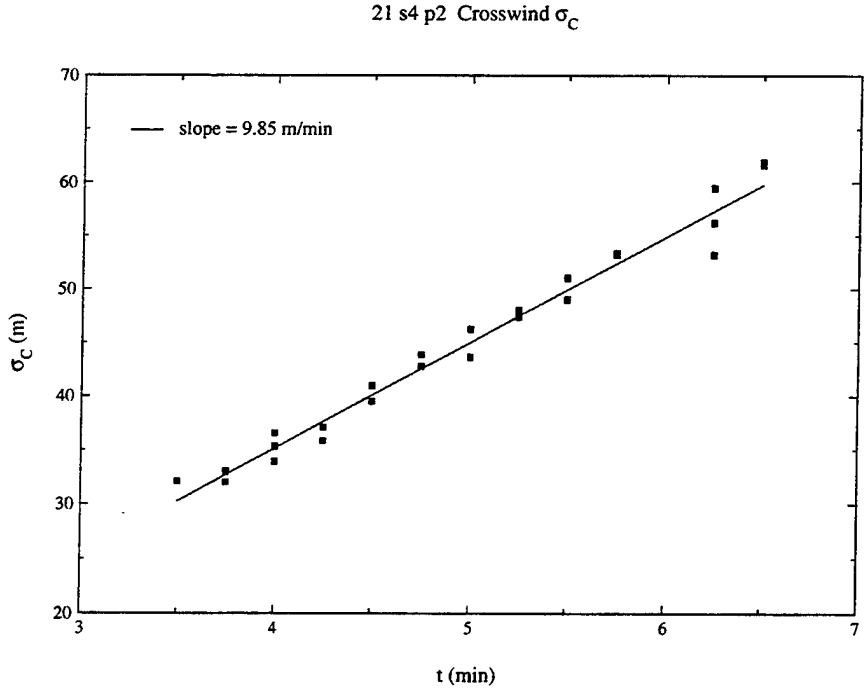

Figure 18: May 21 series 4 puff 2 Crosswind σ

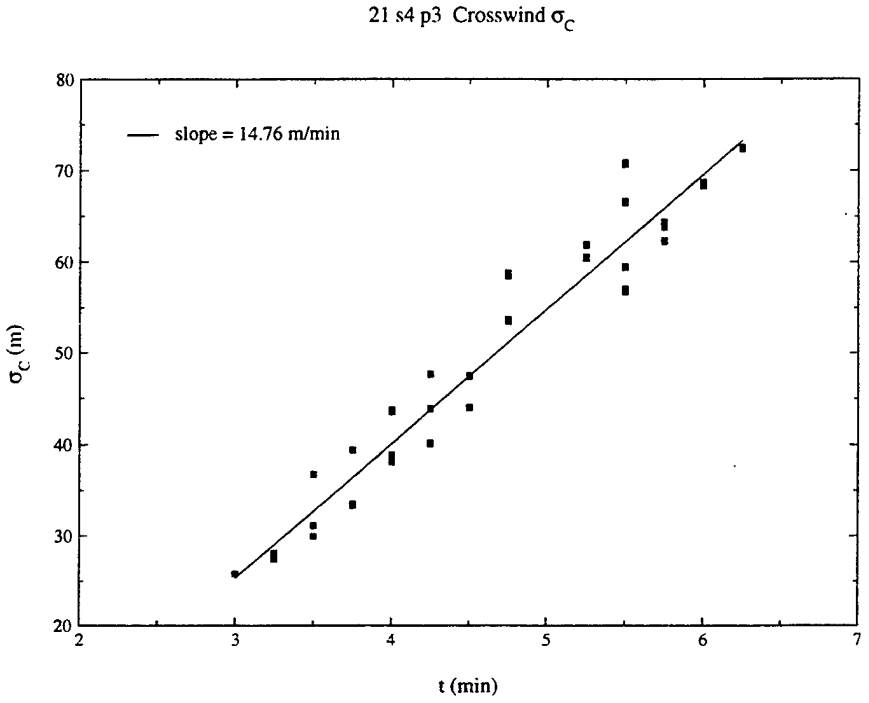

Figure 19: May 21 series 4 puff 3 Crosswind σ

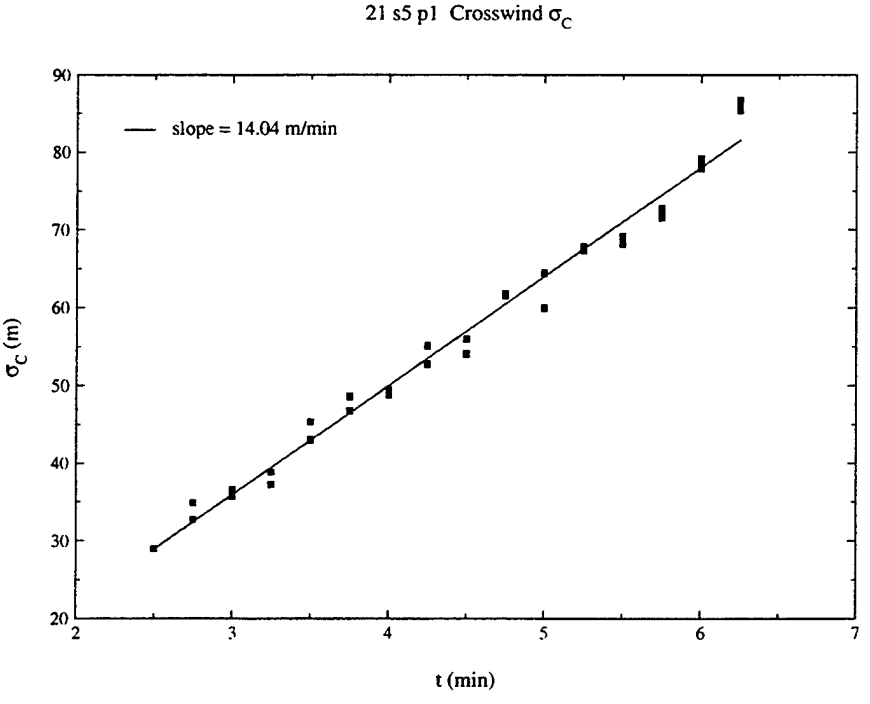

Figure 20: May 21 series 5 puff 1 Crosswind σ

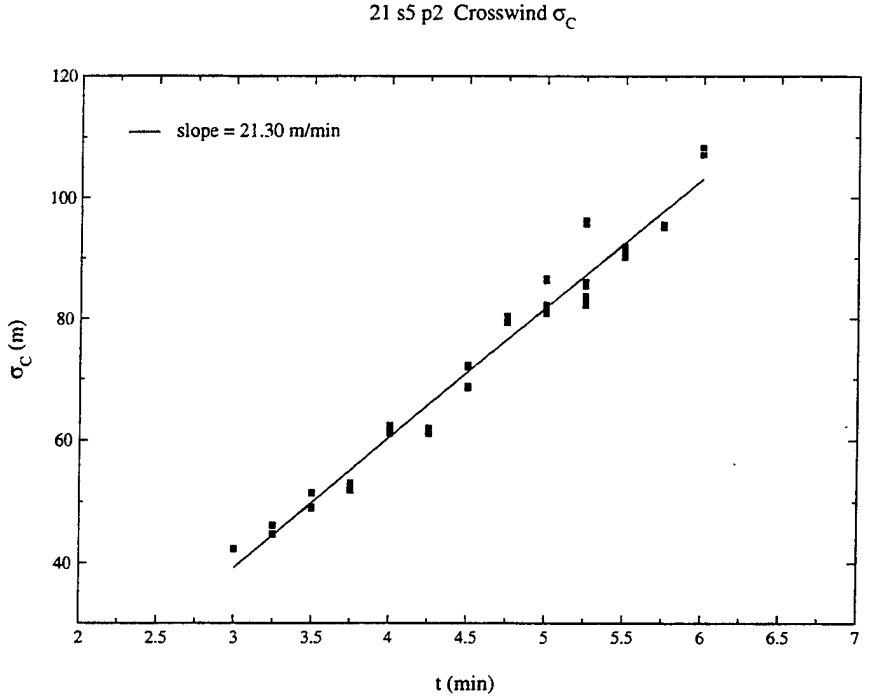

Figure 21: May 21 series 5 puff 2 Crosswind σ

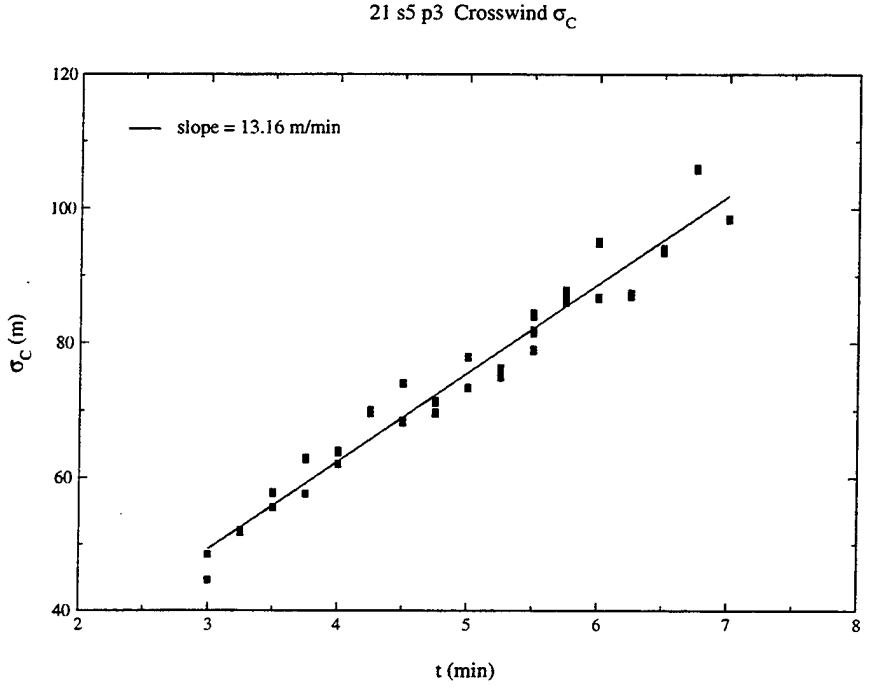

Figure 22: May 21 series 5 puff 3 Crosswind σ

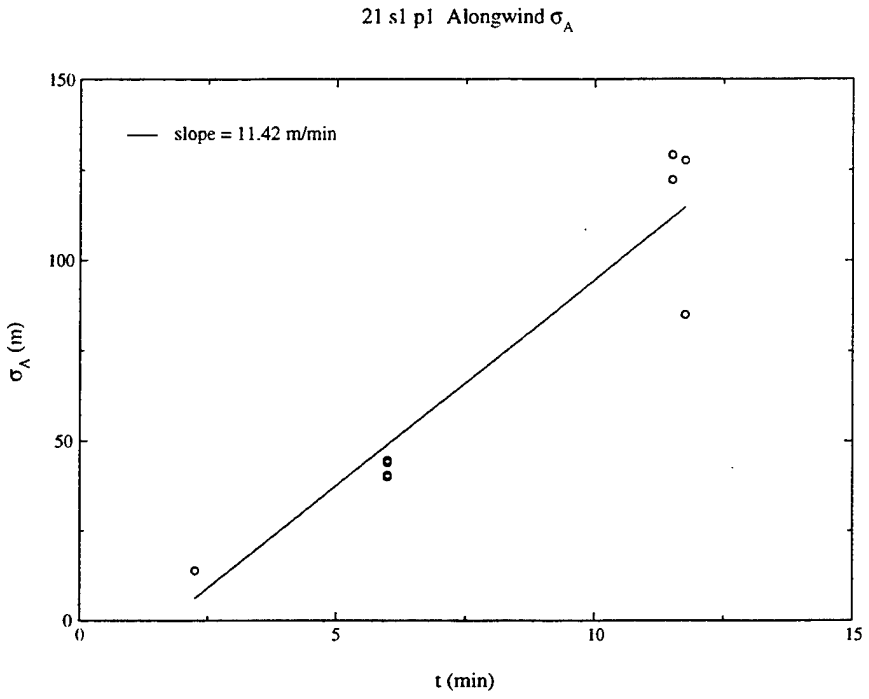

Figure 23: May 21 series 1 puff 1 Alongwind σ

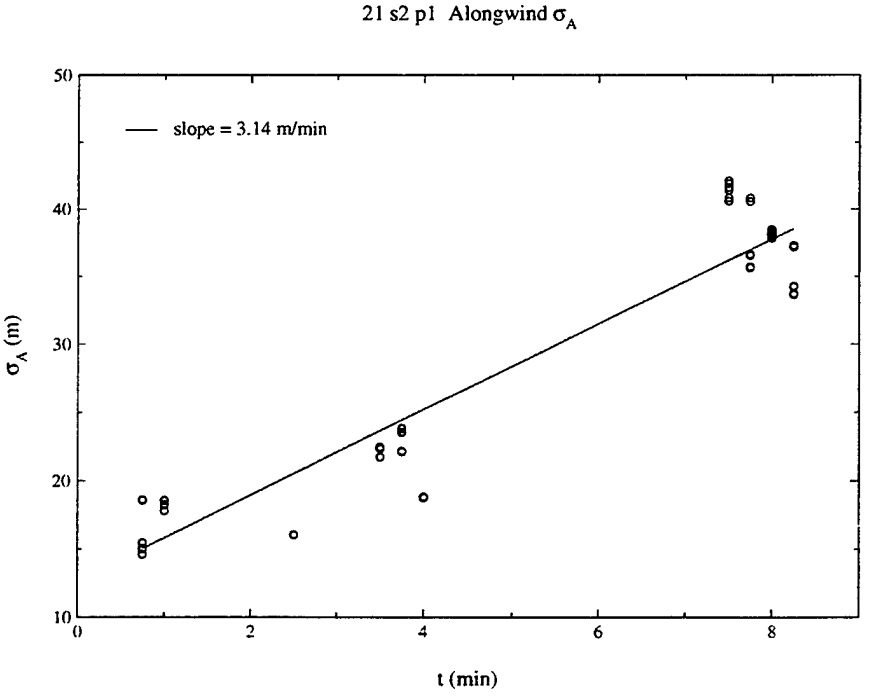

Figure 24: May 21 series 2 puff 1 Alongwind σ

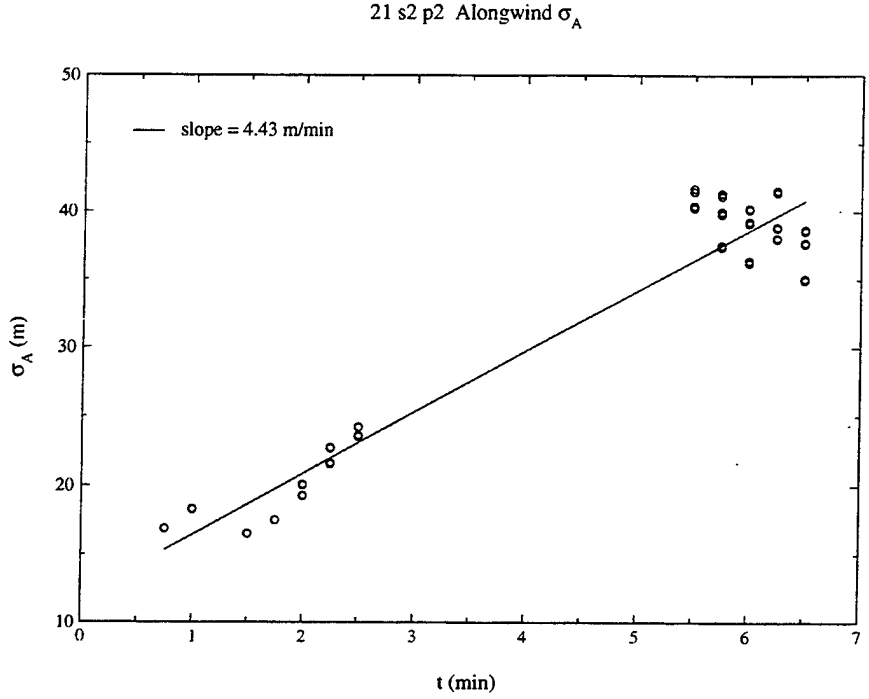

Figure 25: May 21 series 2 puff 2 Alongwind σ

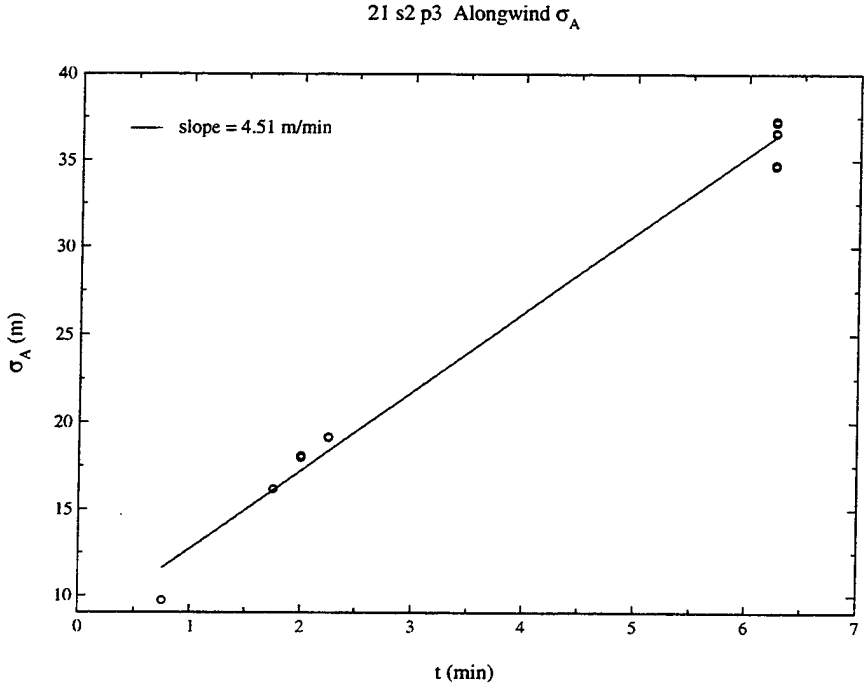

Figure 26: May 21 series 2 puff 3 Alongwind σ

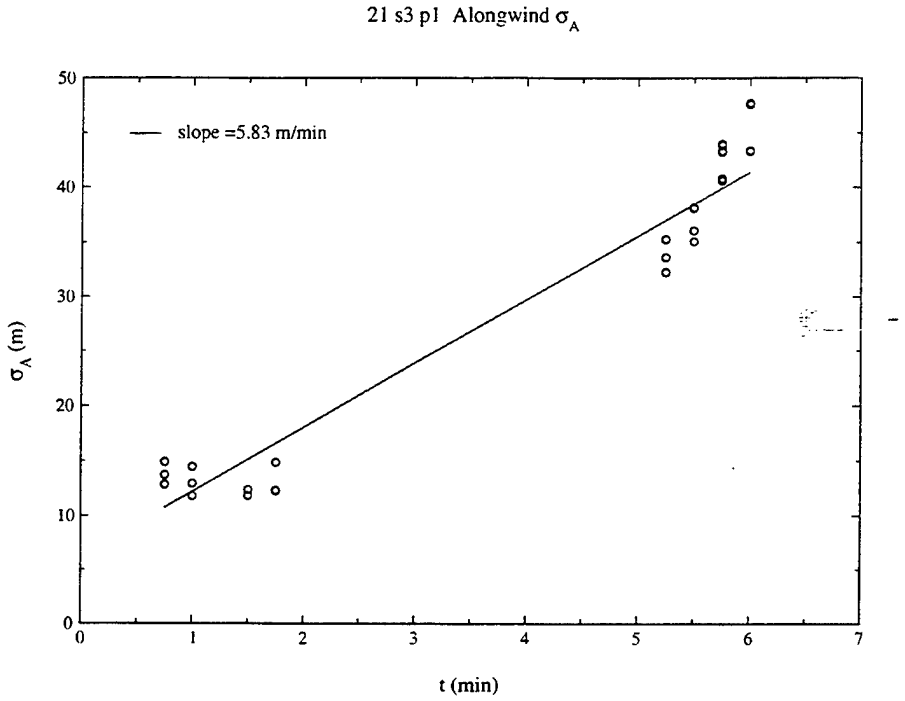

Figure 27: May 21 series 3 puff 1 Alongwind σ

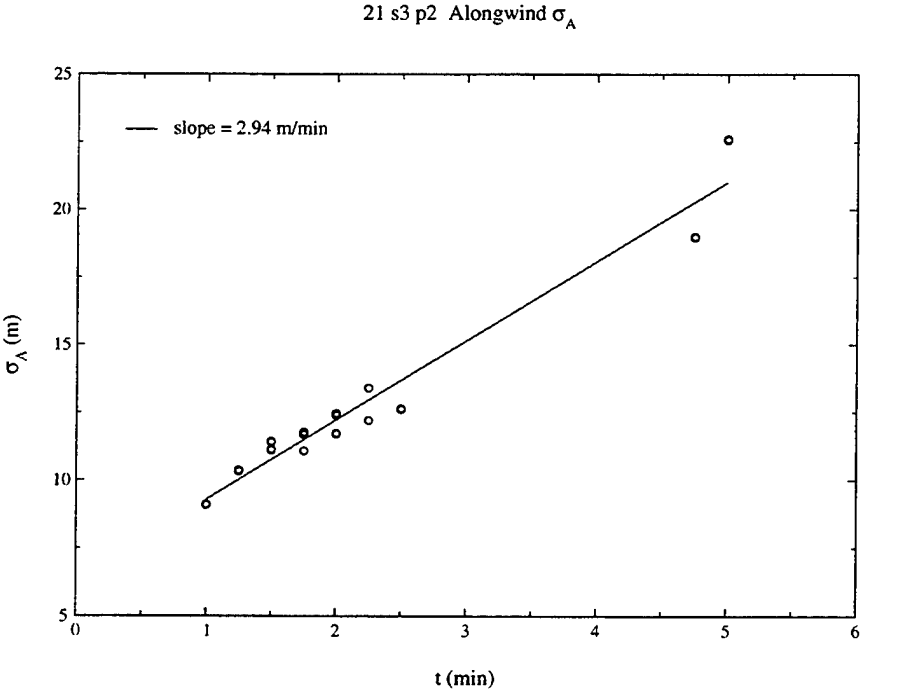

Figure 28: May 21 series 3 puff 2 Alongwind σ

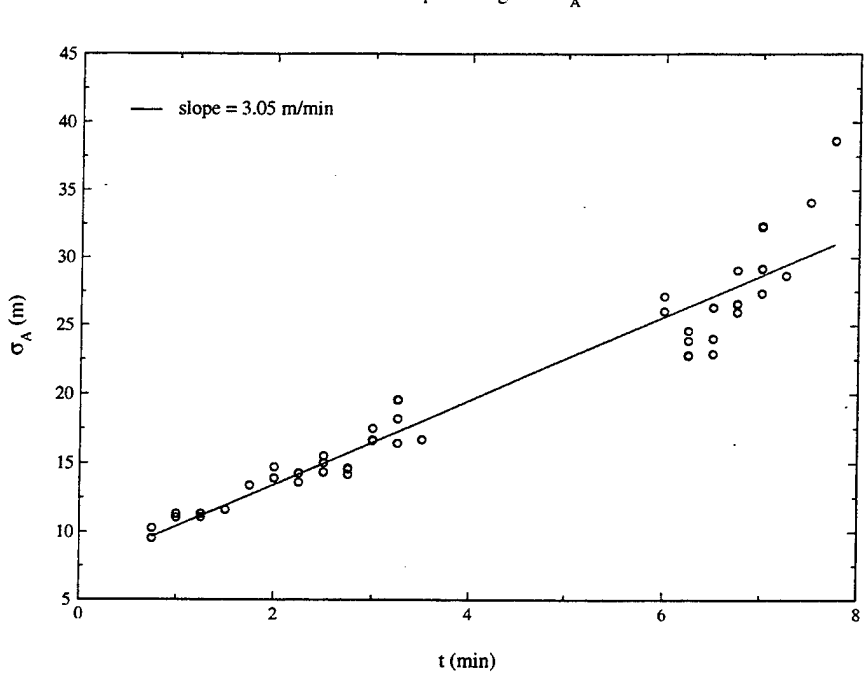

Figure 29: May 21 series 3 puff 3 Alongwind σ

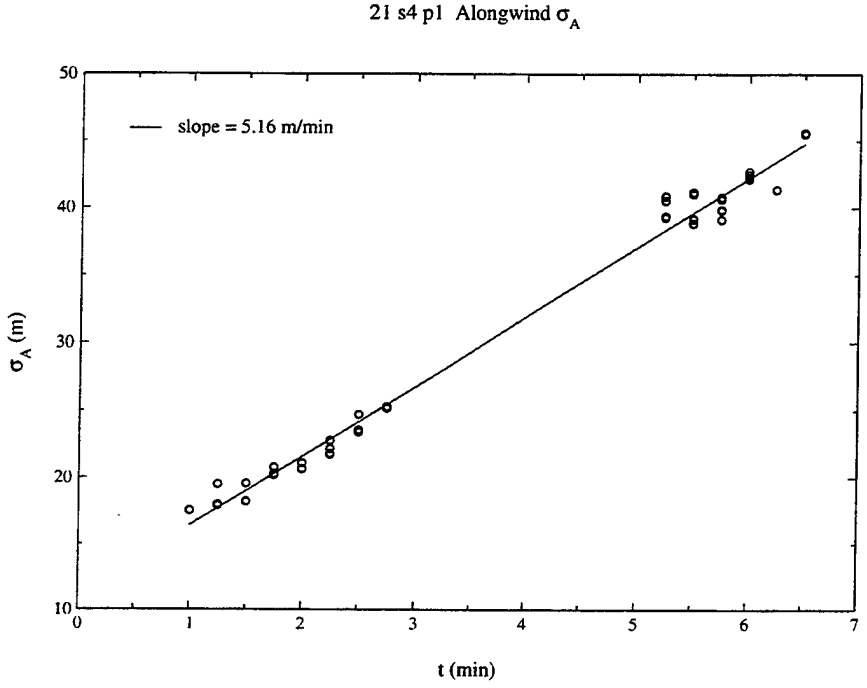

Figure 30: May 21 series 4 puff 1 Alongwind σ

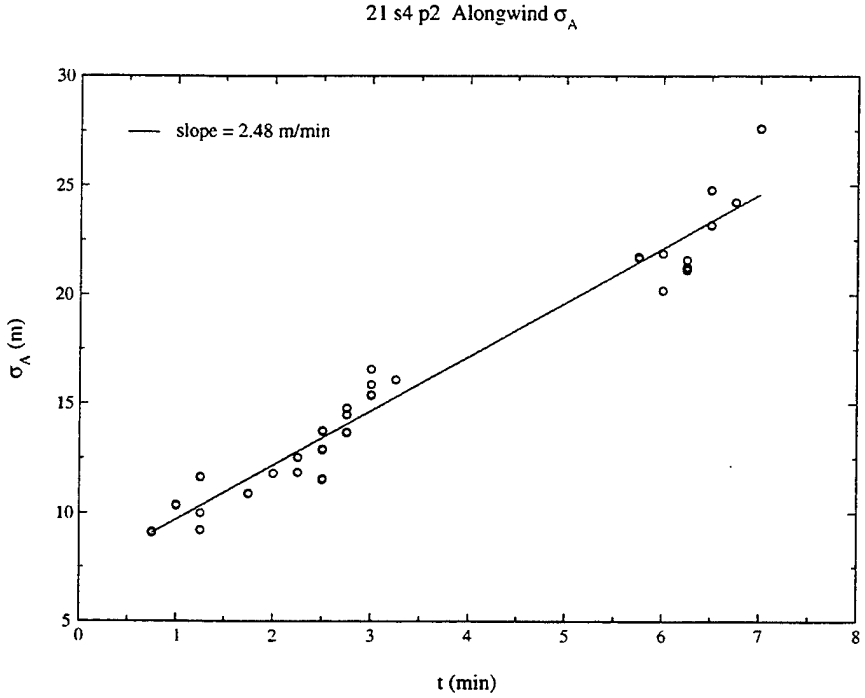

Figure 31: May 21 series 4 puff 2 Alongwind σ

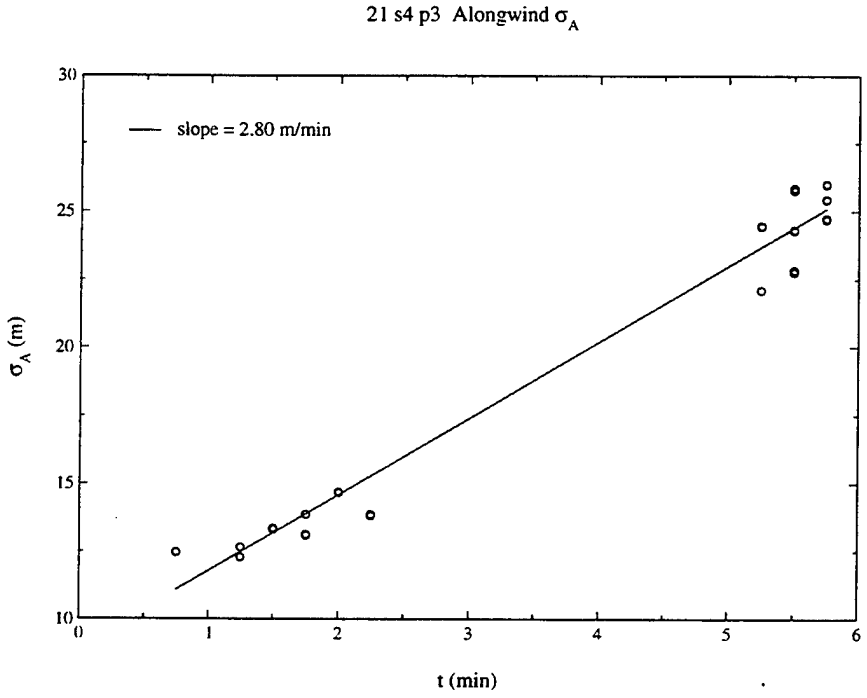

Figure 32: May 21 series 4 puff 3 Alongwind σ

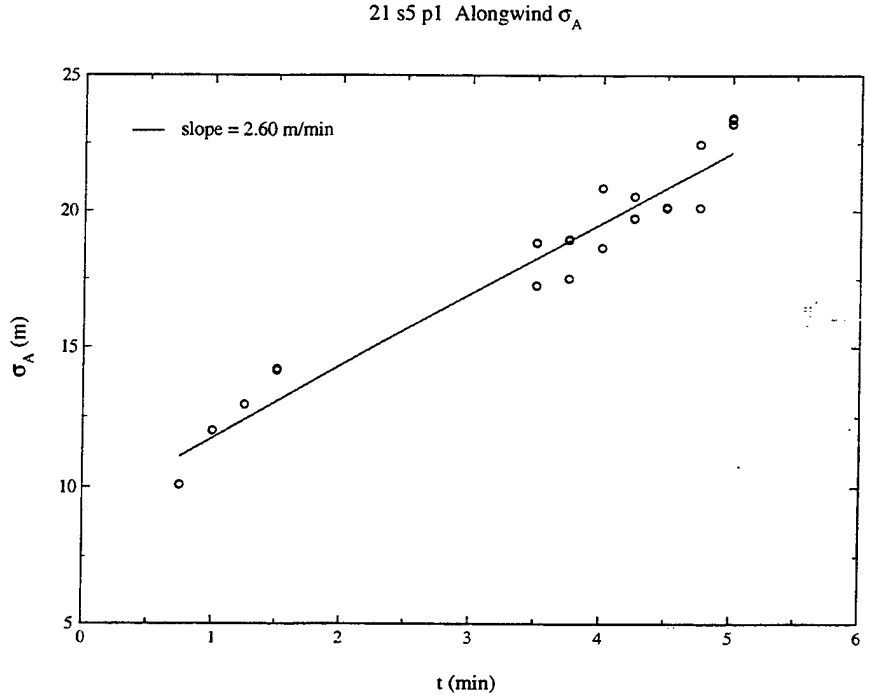

Figure 33: May 21 series 5 puff 1 Alongwind σ

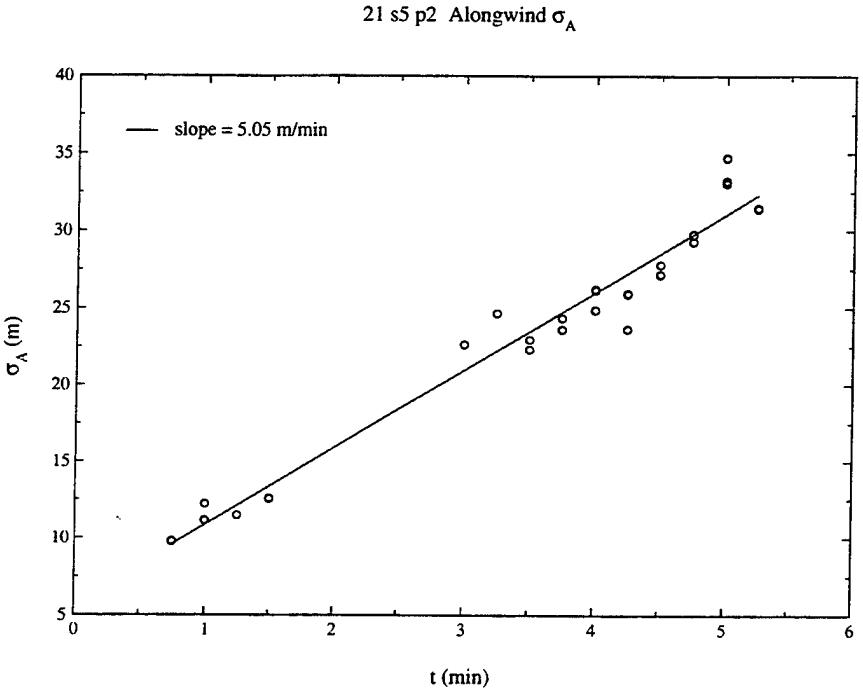

Figure 34: May 21 series 5 puff 2 Alongwind σ

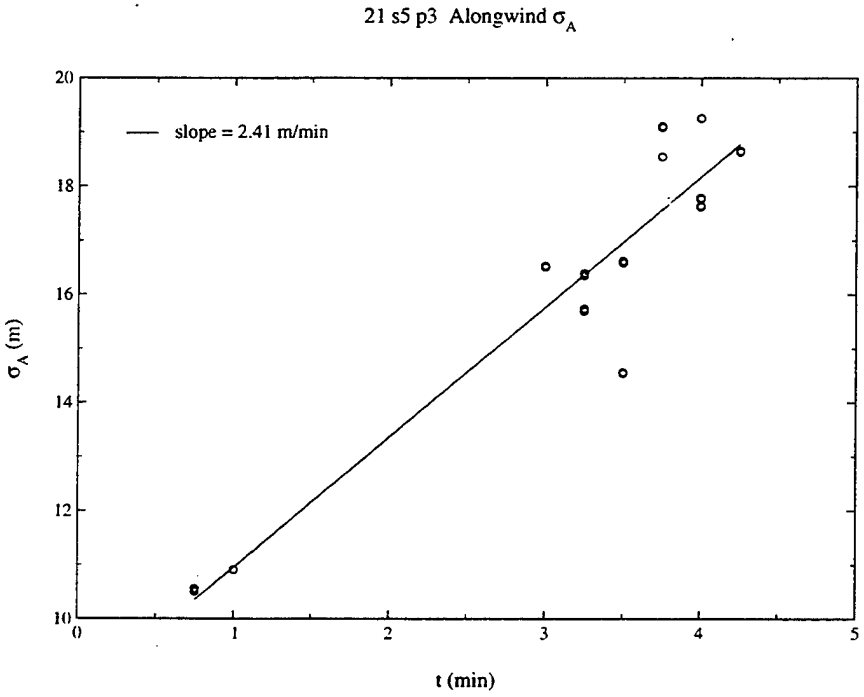

Figure 35: May 21 series 5 puff 3 Alongwind σ

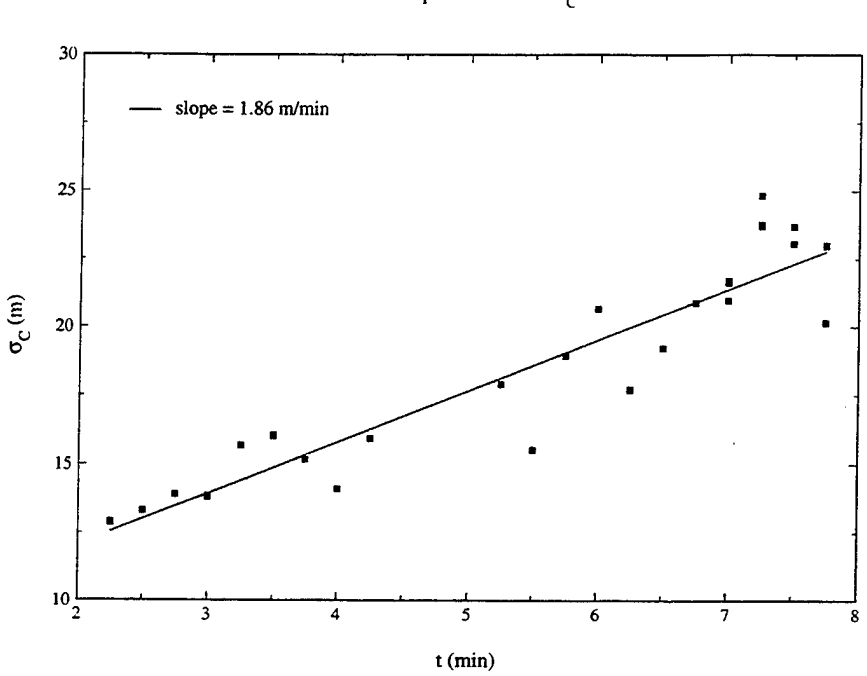

Figure 36: May 23 series 1 puff 1 Crosswind σ

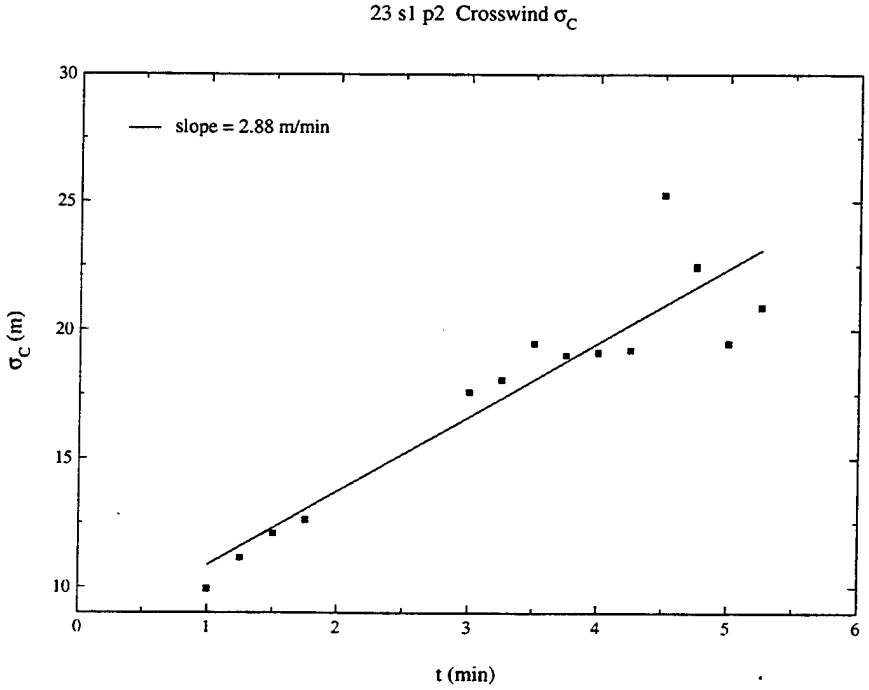

Figure 37: May 23 series 1 puff 2 Crosswind σ

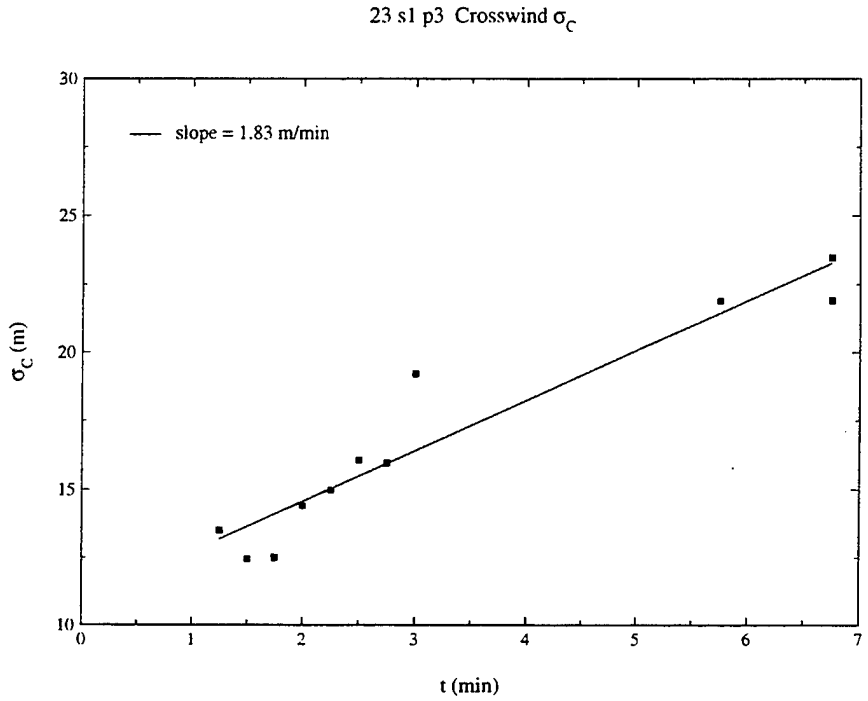

Figure 38: May 23 series 1 puff 3 Crosswind σ

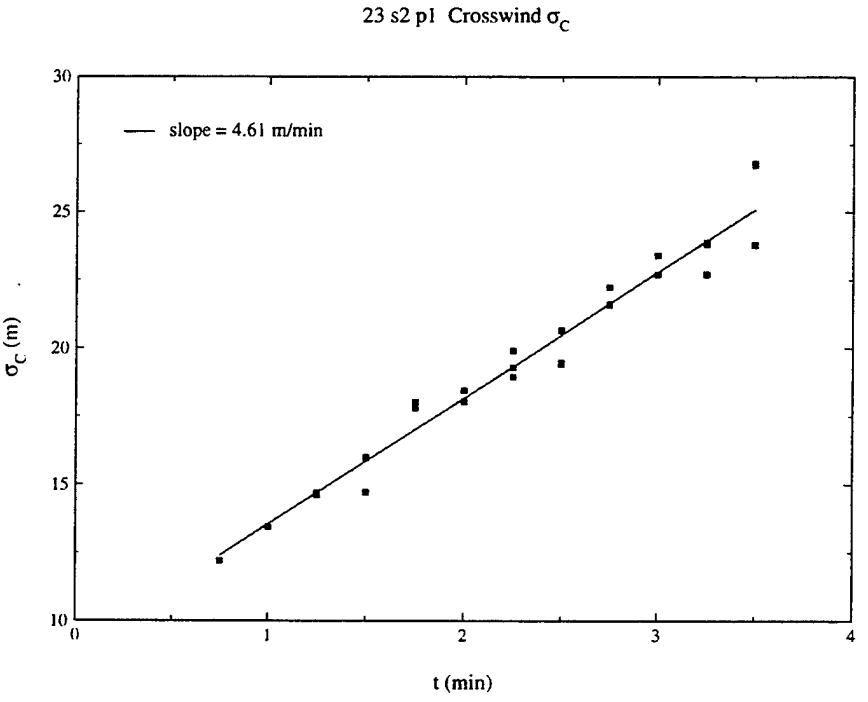

Figure 39: May 23 series 2 puff 1 Crosswind σ

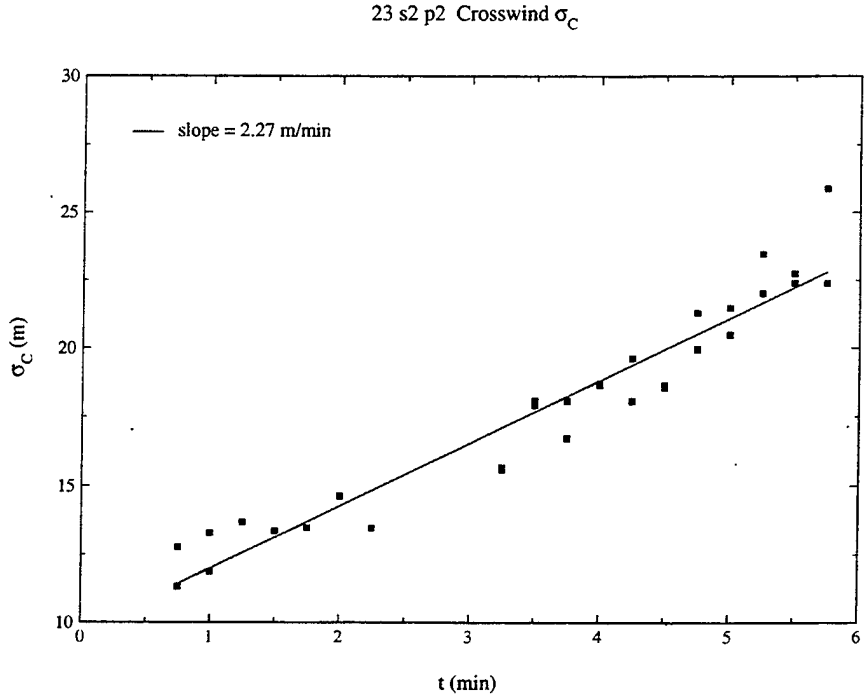

Figure 40: May 23 series 2 puff 2 Crosswind σ

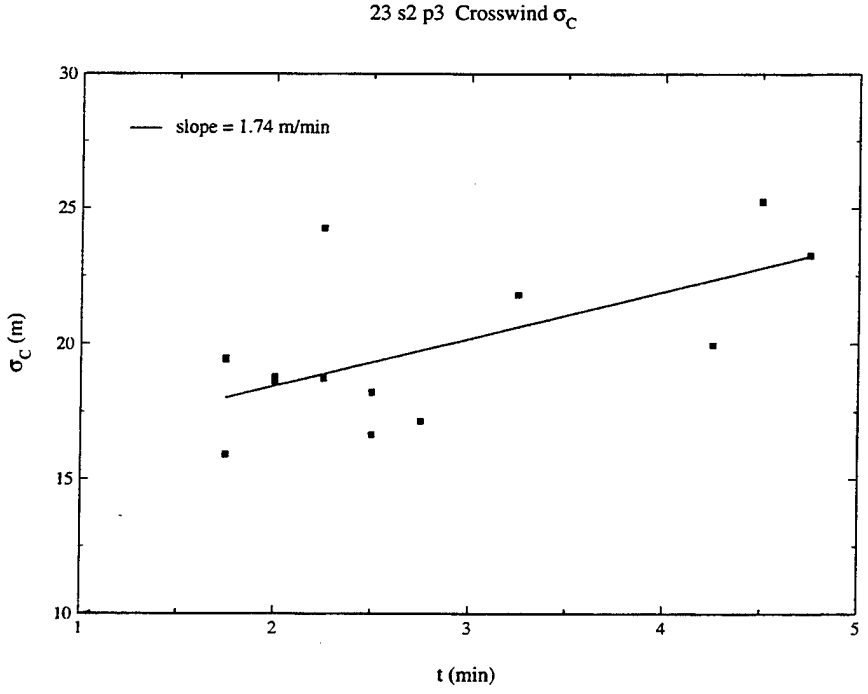

Figure 41: May 23 series 2 puff 3 Crosswind σ

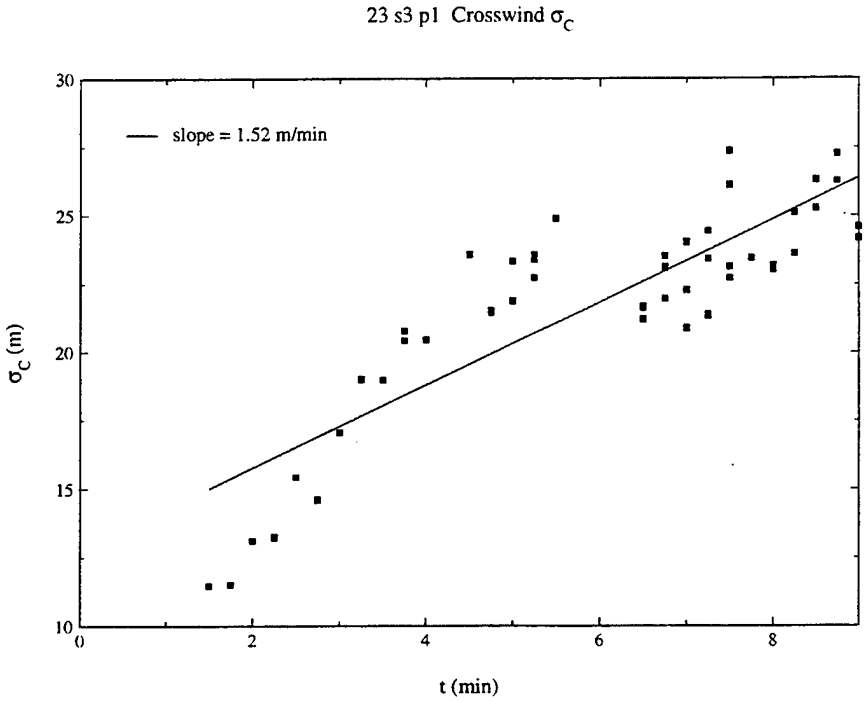

Figure 42: May 23 series 3 puff 1 Crosswind σ

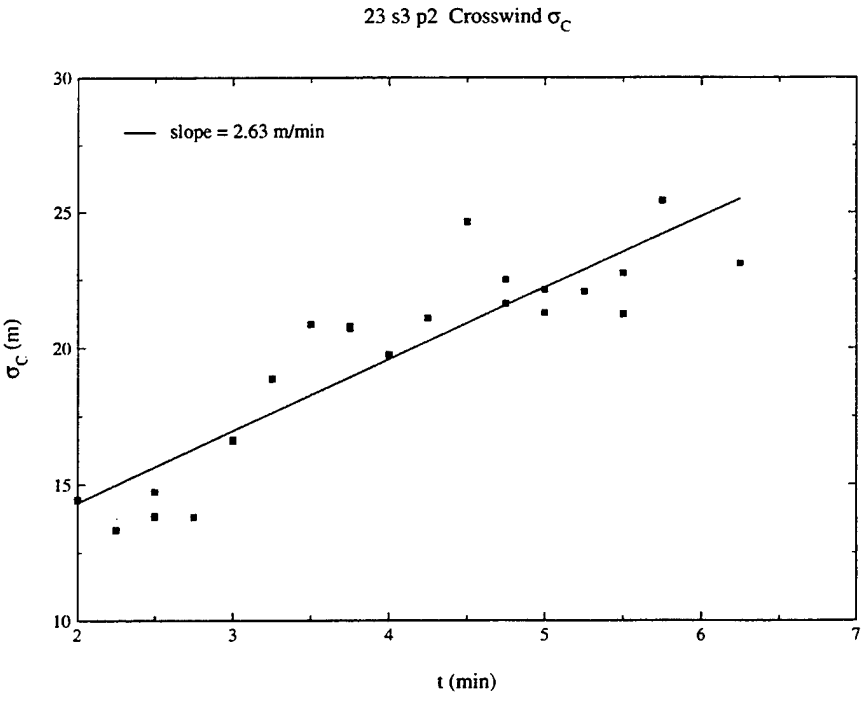

Figure 43: May 23 series 3 puff 2 Crosswind σ

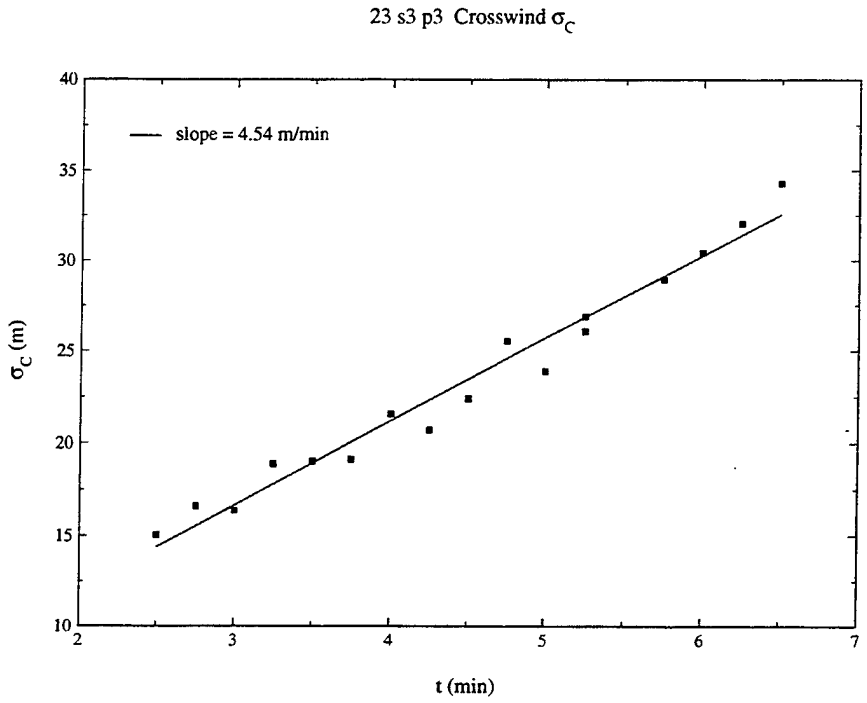

Figure 44: May 23 series 3 puff 3 Crosswind σ

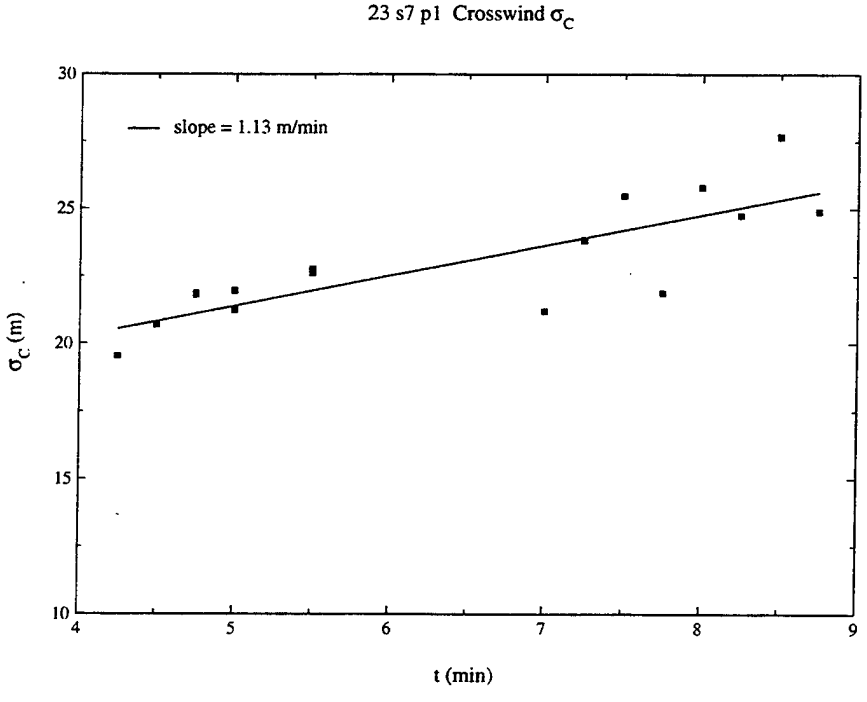

Figure 45: May 23 series 7 puff 1 Crosswind σ

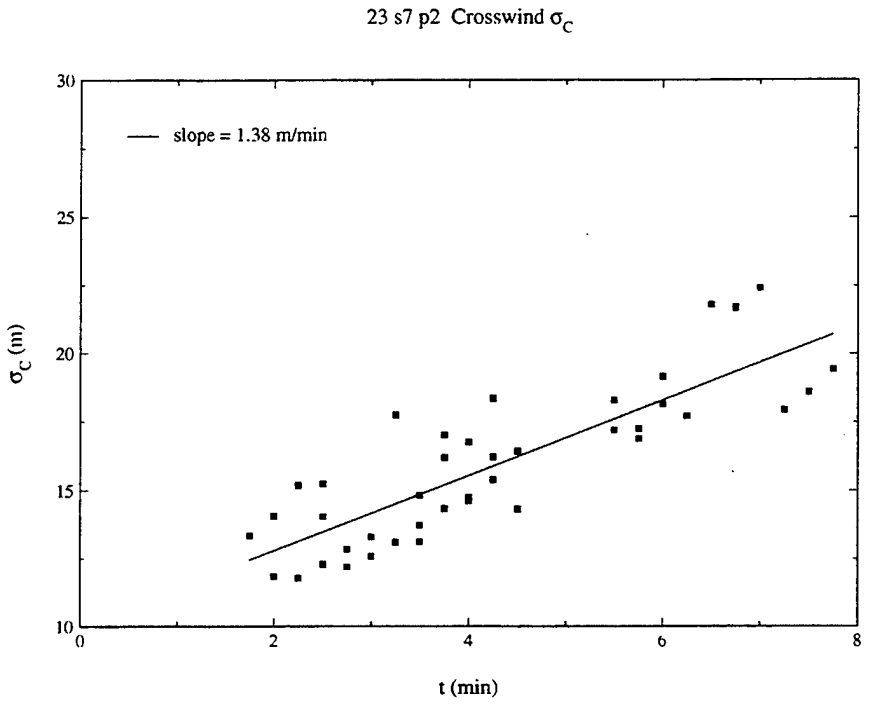

Figure 46: May 23 series 7 puff 2 Crosswind σ

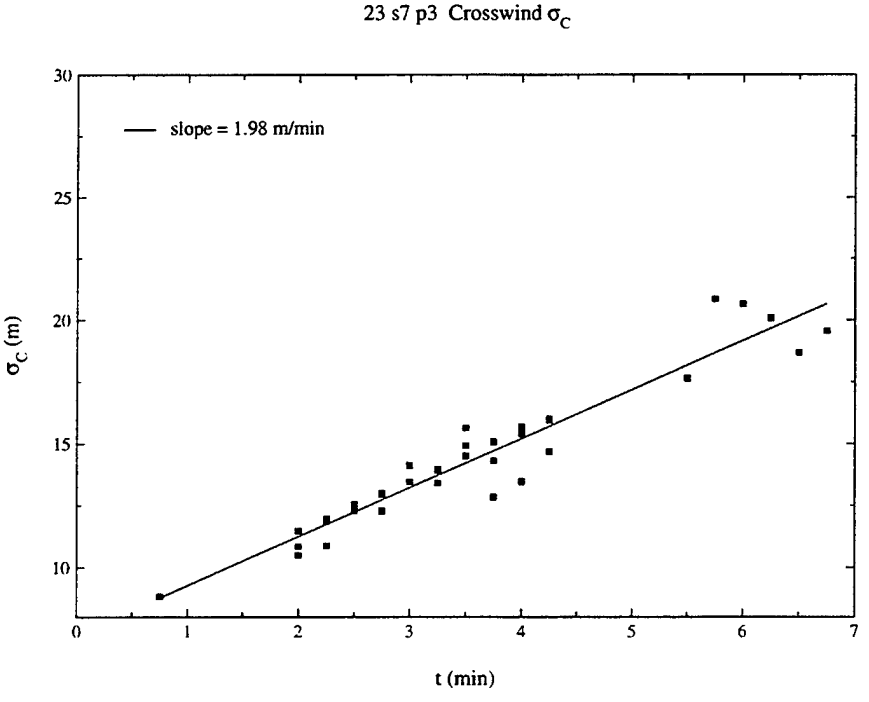

Figure 47: May 23 series 7 puff 3 Crosswind σ

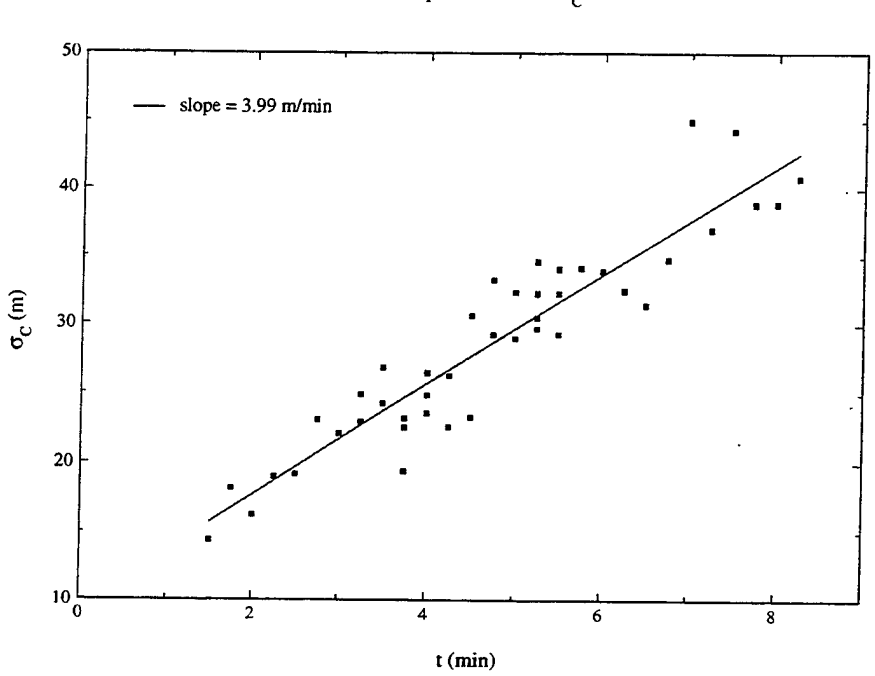

Figure 48: May 23 series 8 puff 1 Crosswind σ

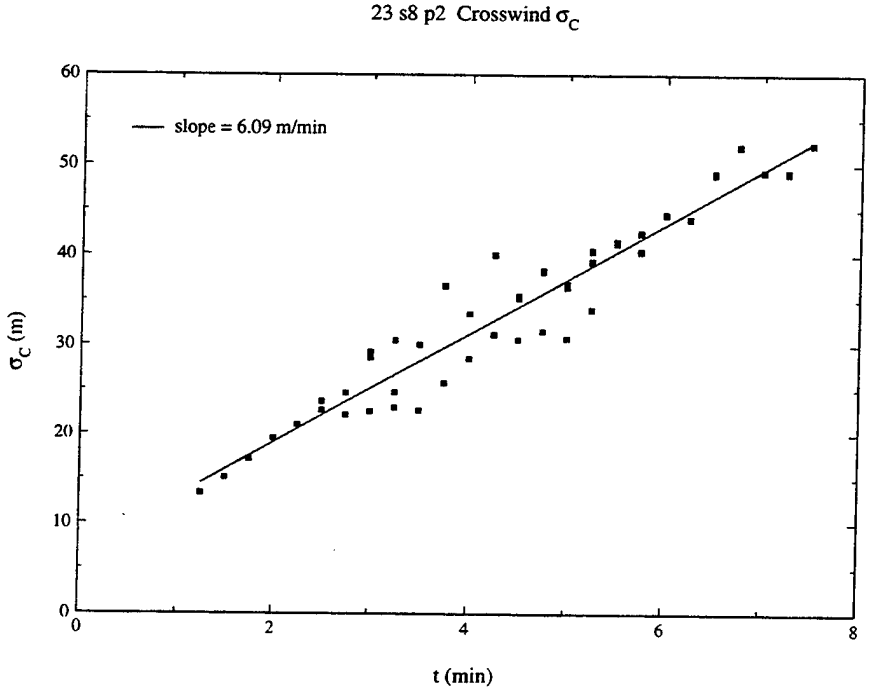

Figure 49: May 23 series 8 puff 2 Crosswind σ

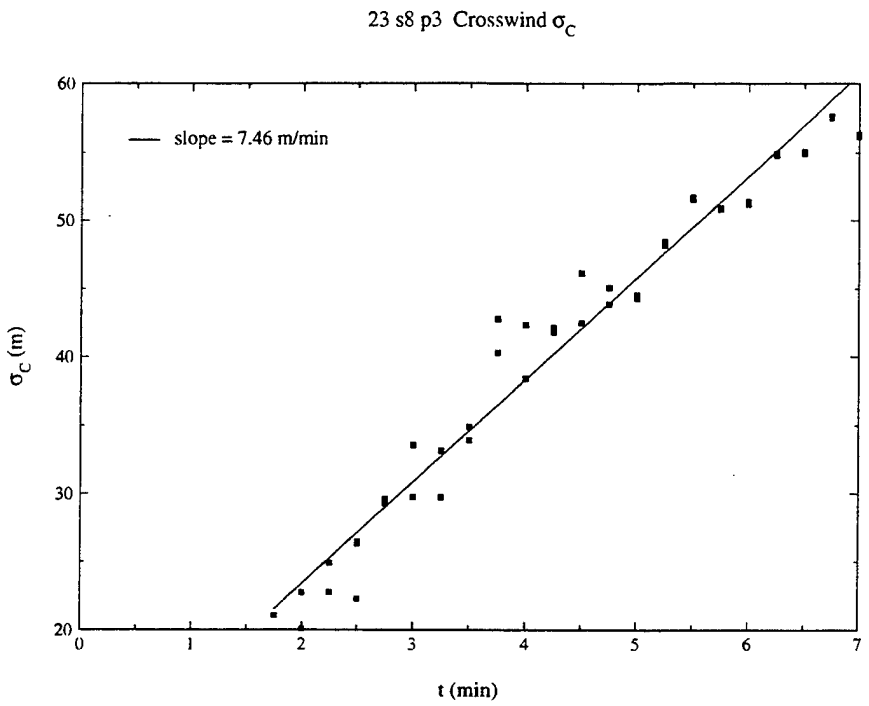

Figure 50: May 23 series 8 puff 3 Crosswind σ

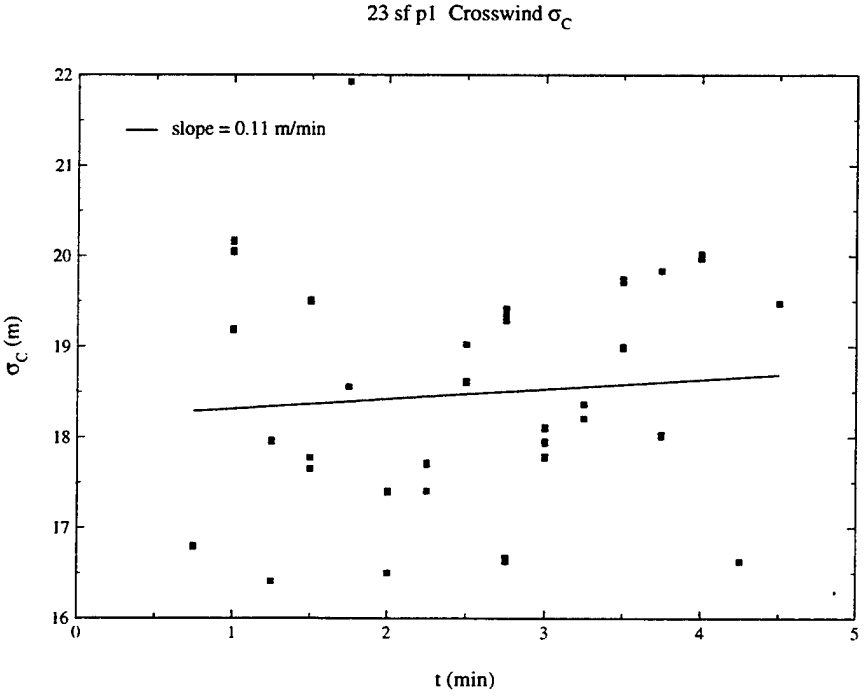

Figure 51: May 23 series f puff 1 Crosswind σ

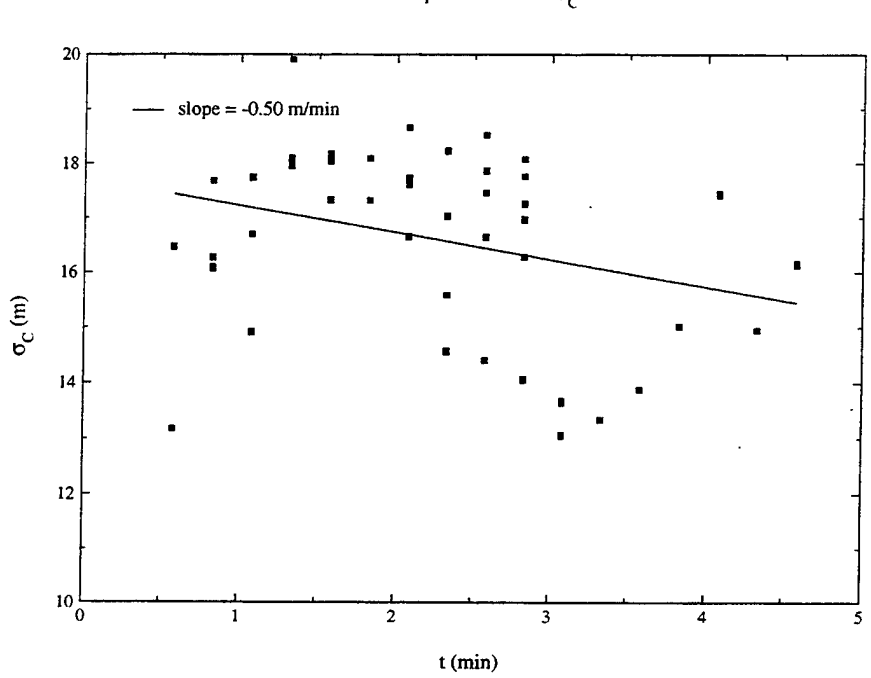

Figure 52: May 23 series f puff 2 Crosswind σ

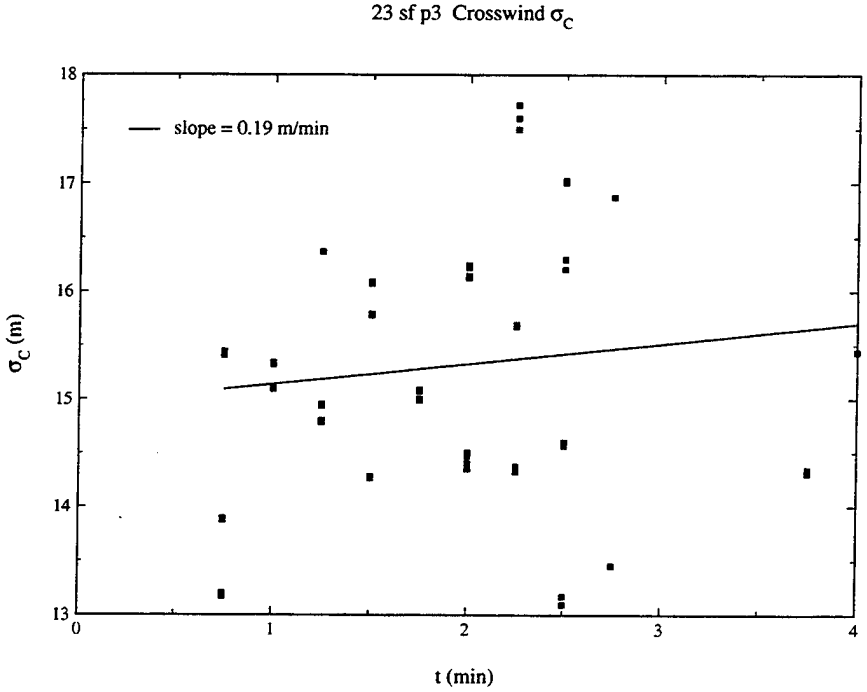

Figure 53: May 23 series f puff 3 Crosswind σ

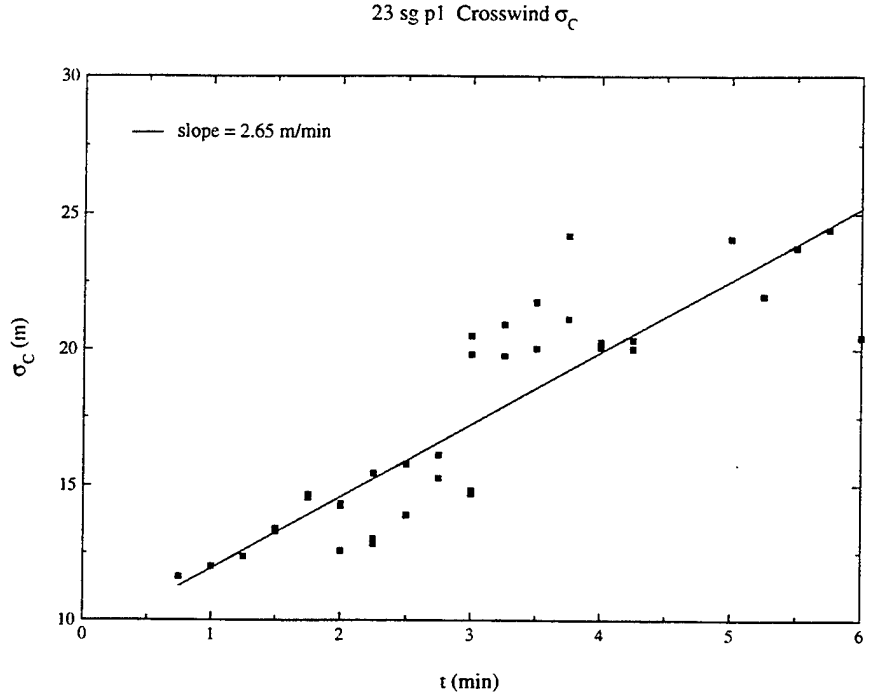

Figure 54: May 23 series g puff 1 Crosswind σ

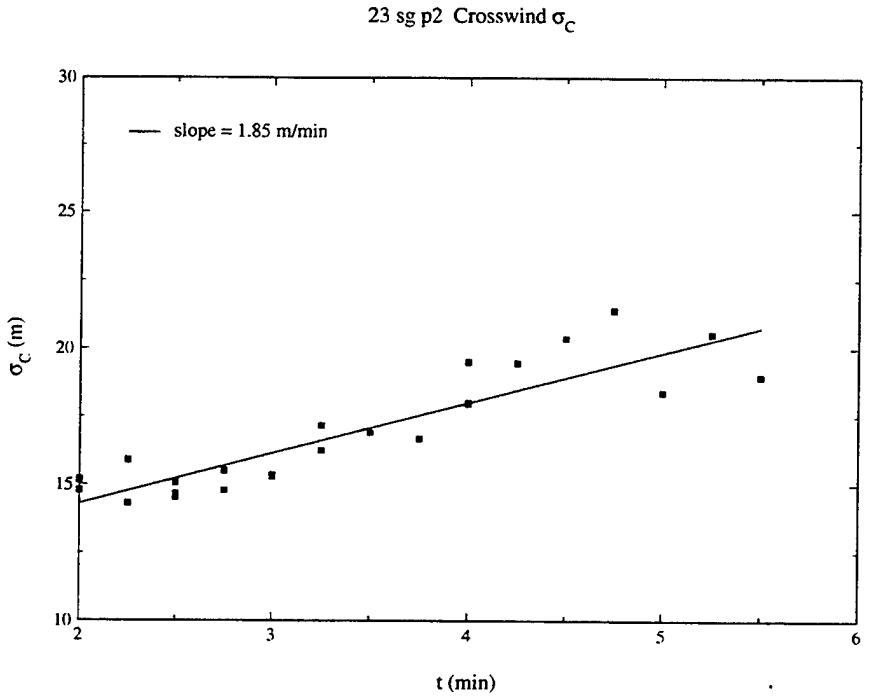

Figure 55: May 23 series g puff 2 Crosswind σ

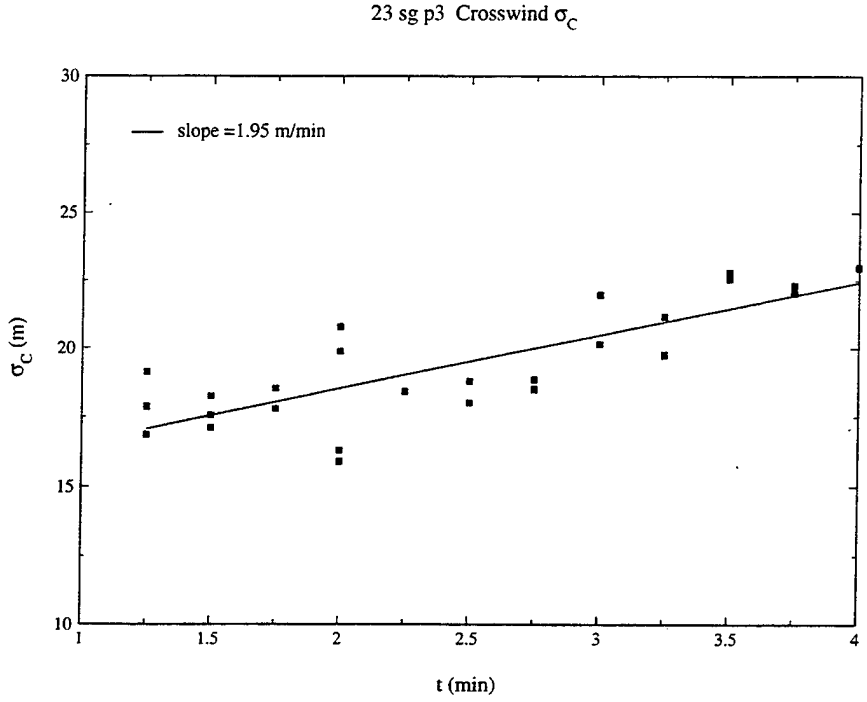

Figure 56: May 23 series g puff 3 Crosswind σ

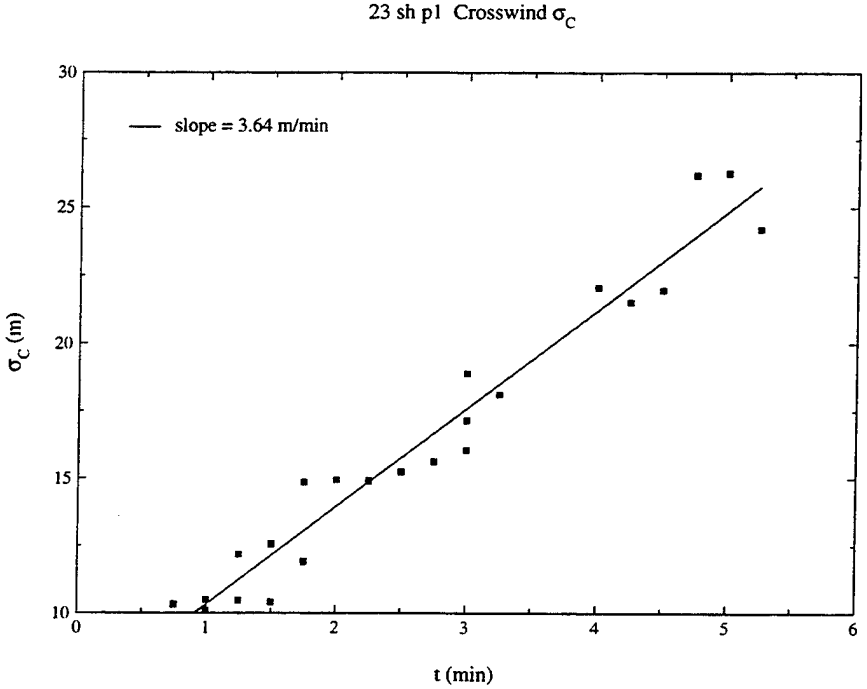

Figure 57: May 23 series h puff 1 Crosswind σ

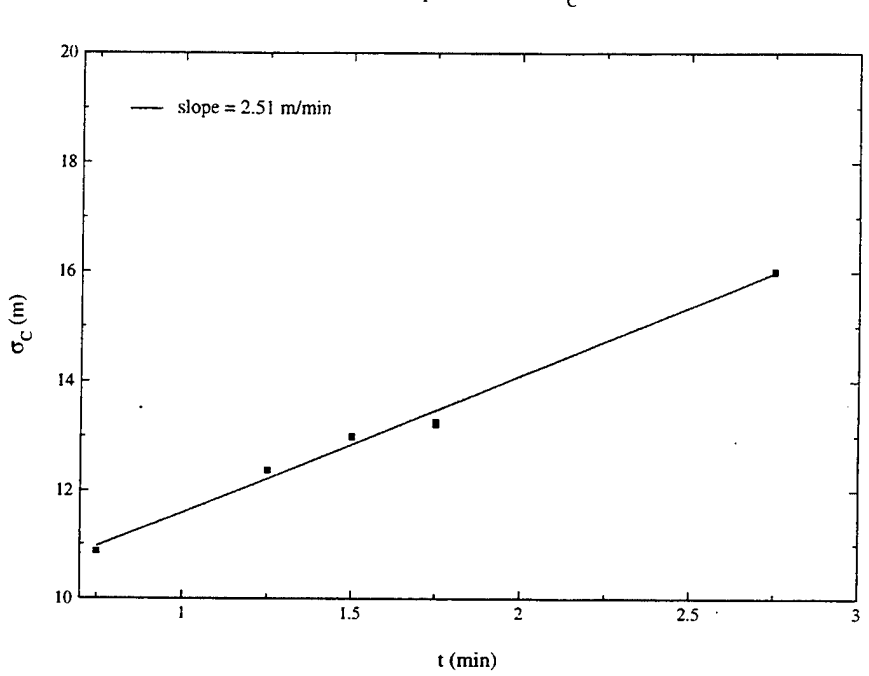

Figure 58: May 23 series h puff 2 Crosswind σ

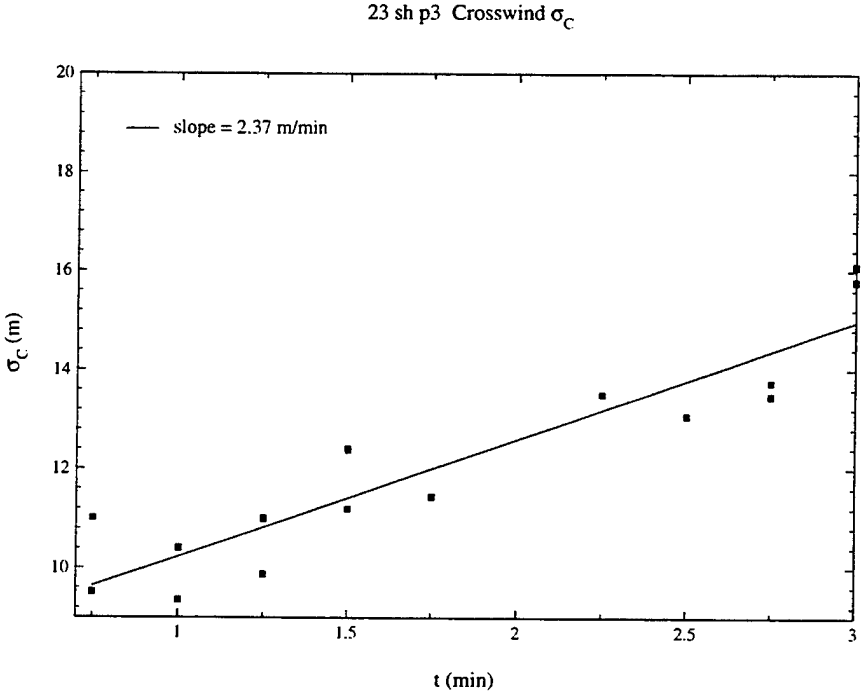

Figure 59: May 23 series h puff 3 Crosswind σ

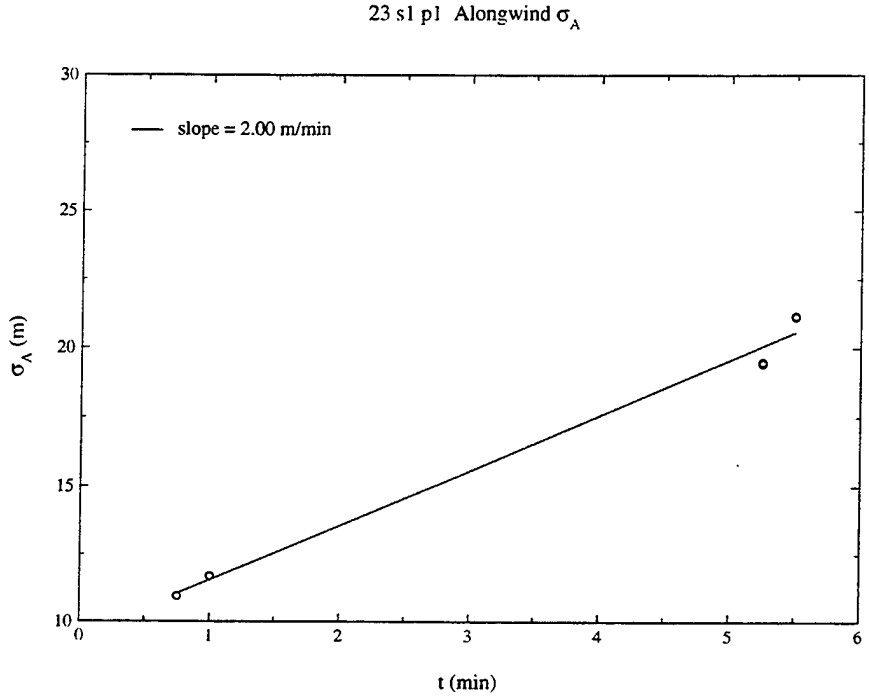

Figure 60: May 23 series 1 puff 1 Alongwind σ

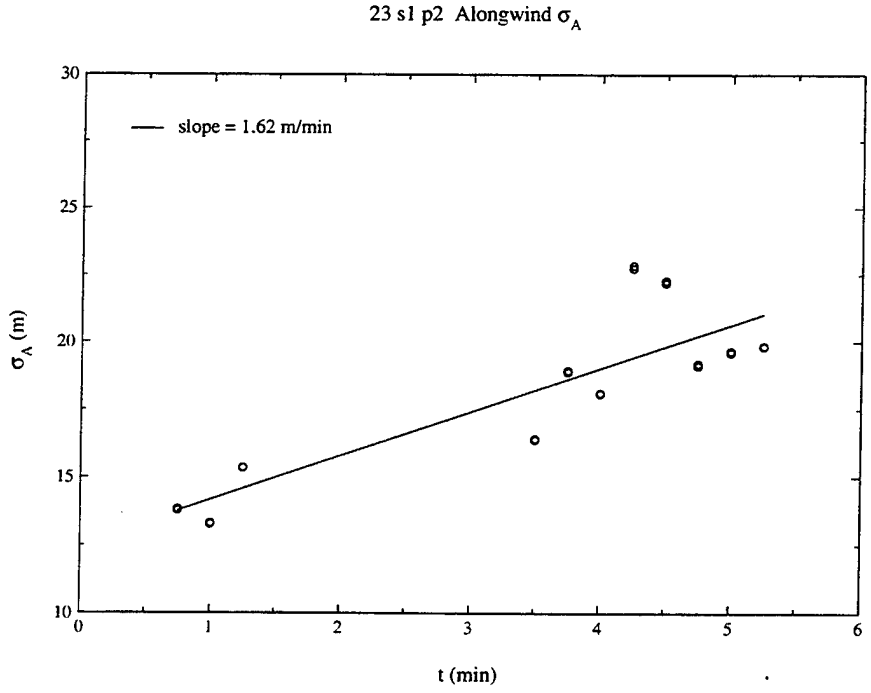

Figure 61: May 23 series 1 puff 2 Alongwind σ

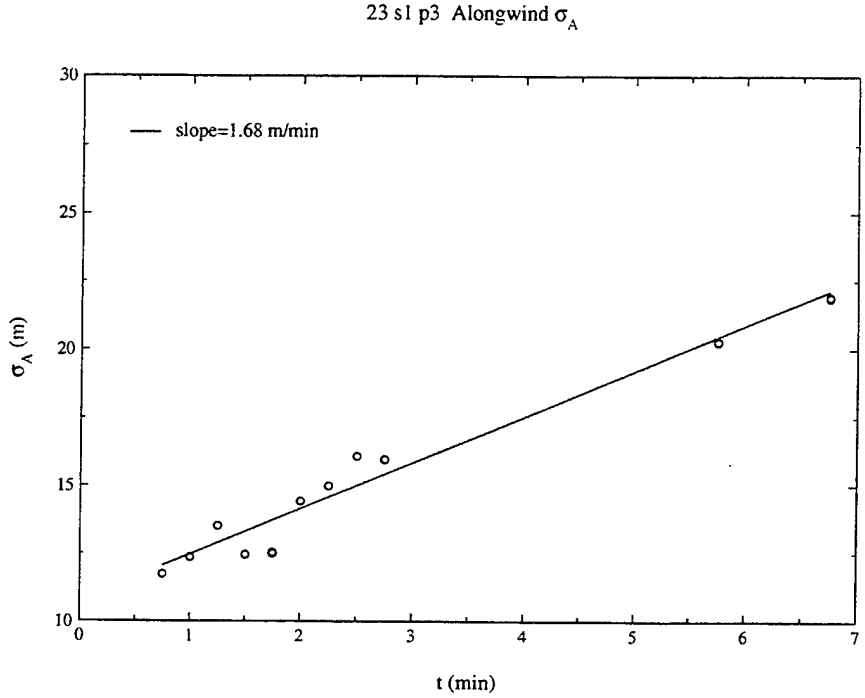

Figure 62: May 23 series 1 puff 3 Alongwind σ

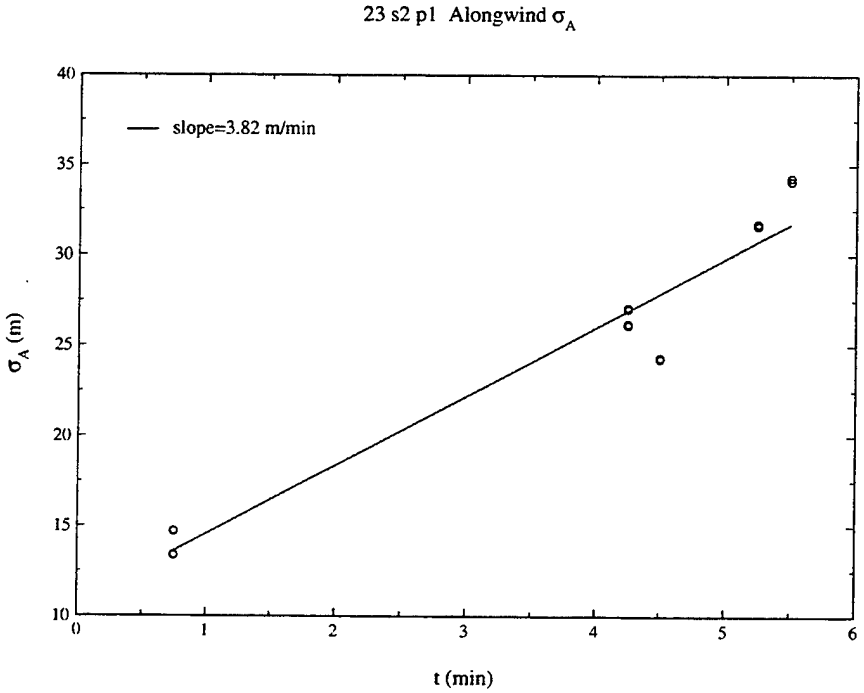

Figure 63: May 23 series 2 puff 1 Alongwind σ

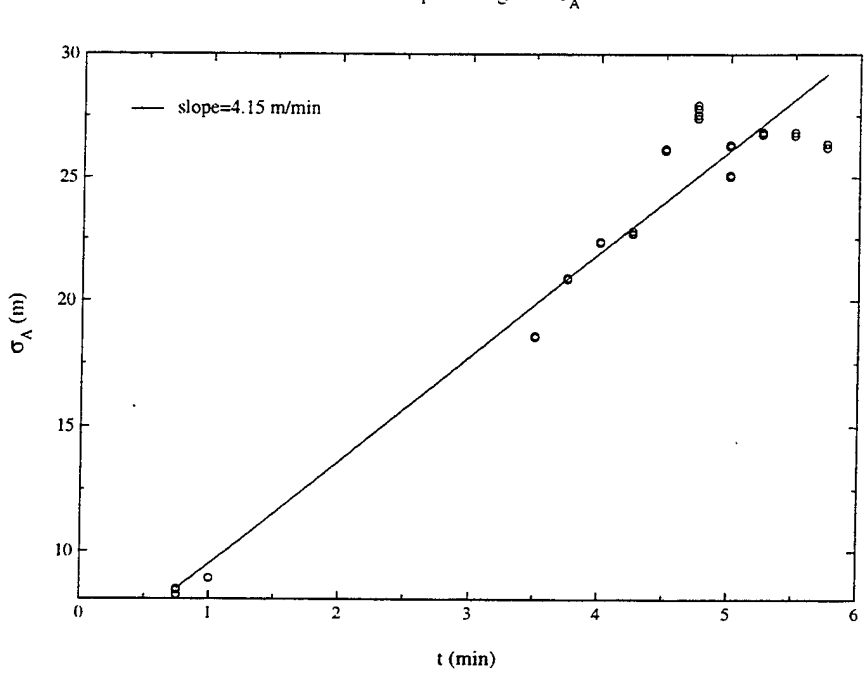

Figure 64: May 23 series 2 puff 2 Alongwind σ

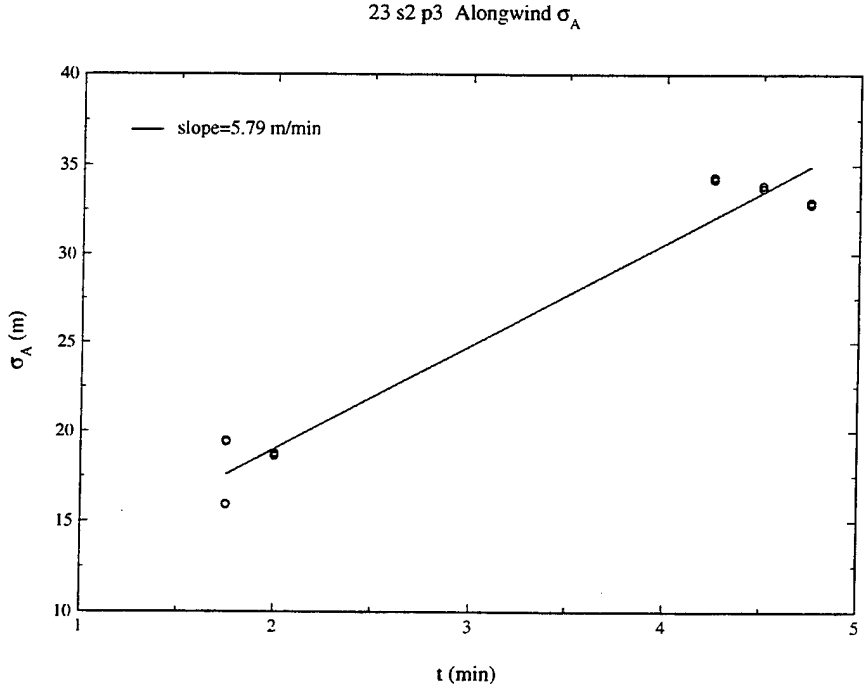

Figure 65: May 23 series 2 puff 3 Alongwind σ

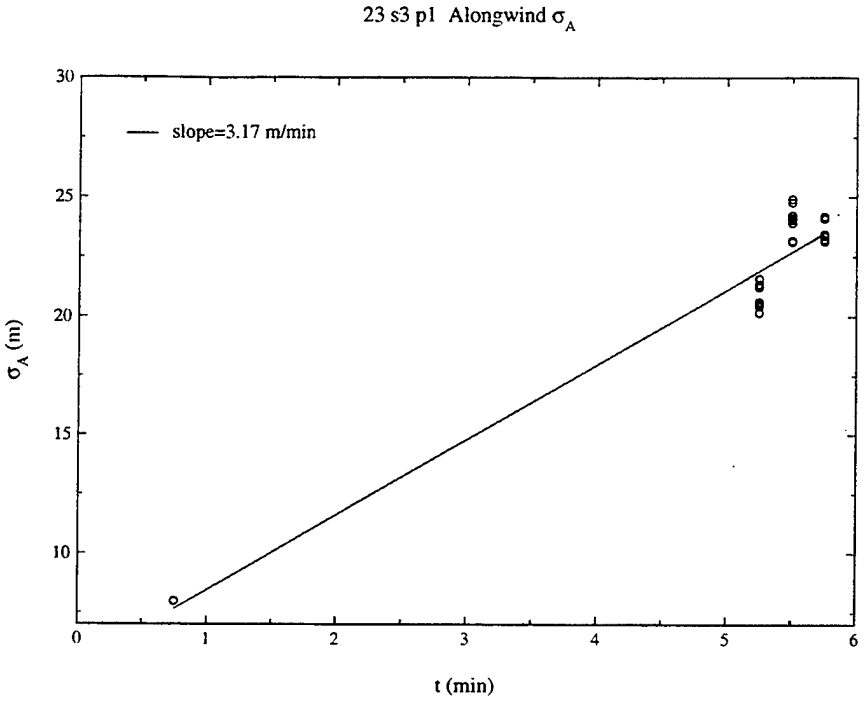

Figure 66: May 23 series 3 puff 1 Alongwind σ

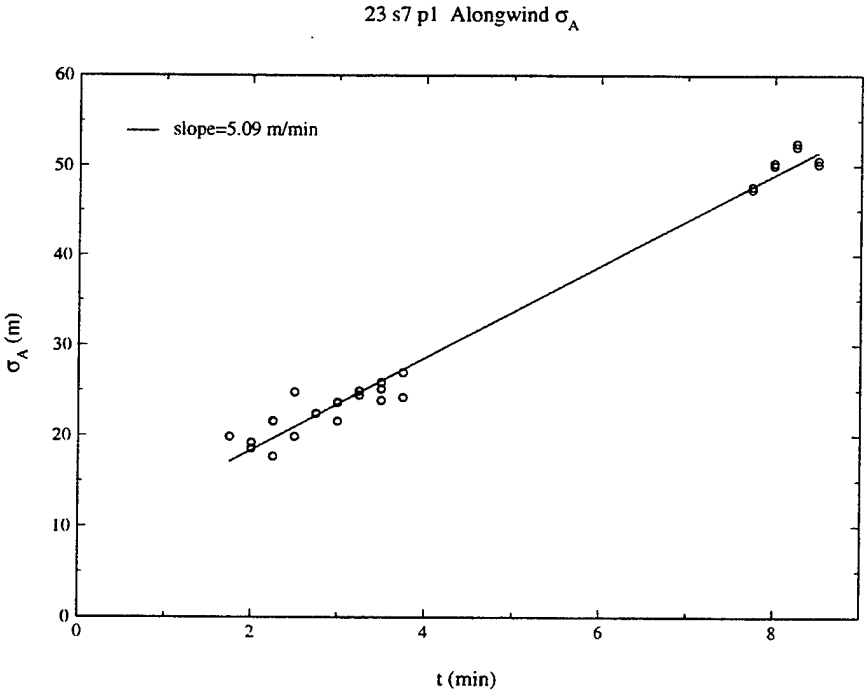

Figure 67: May 23 series 7 puff 1 Alongwind σ

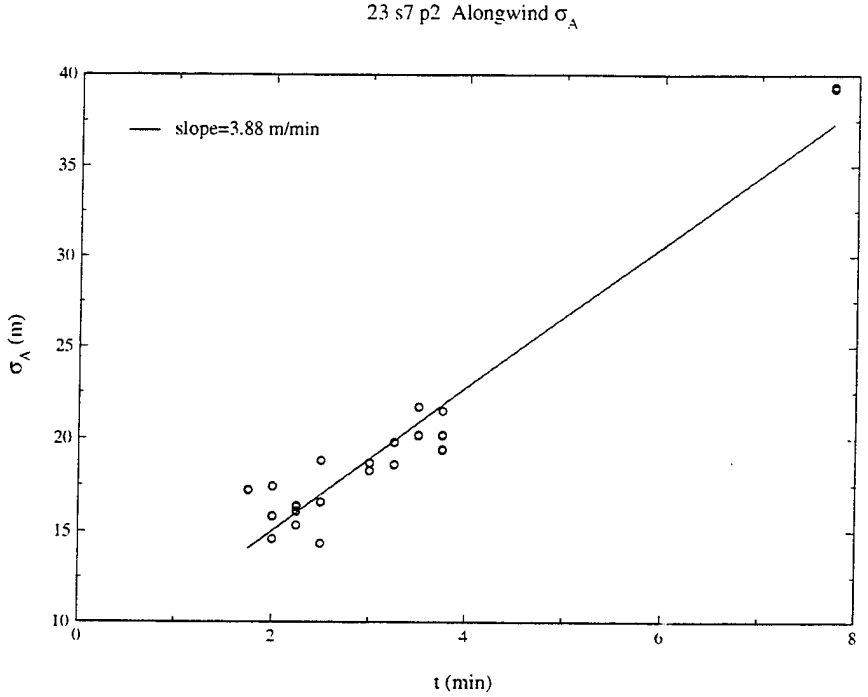

Figure 68: May 23 series 7 puff 2 Alongwind σ

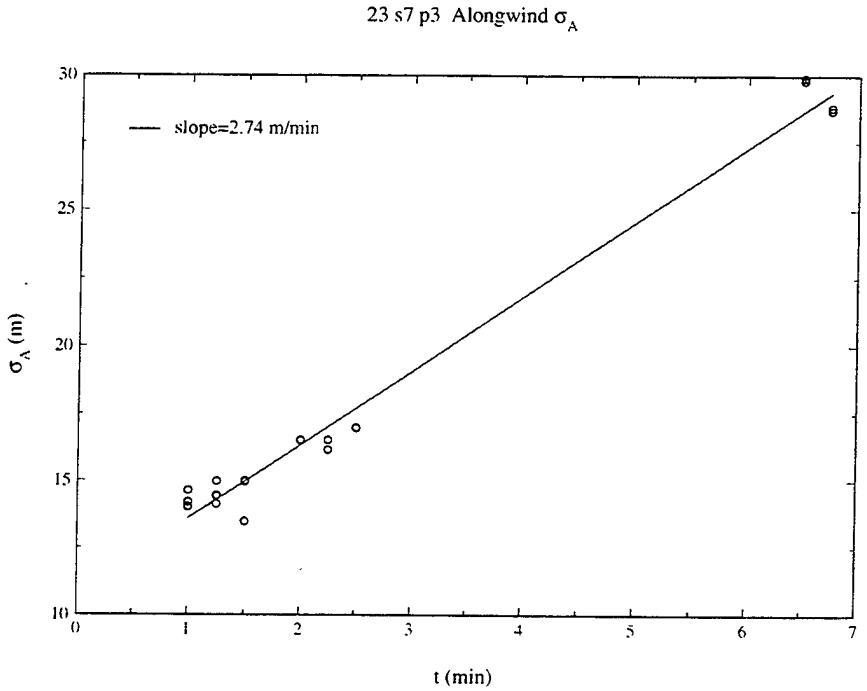

Figure 69: May 23 series 7 puff 3 Alongwind σ

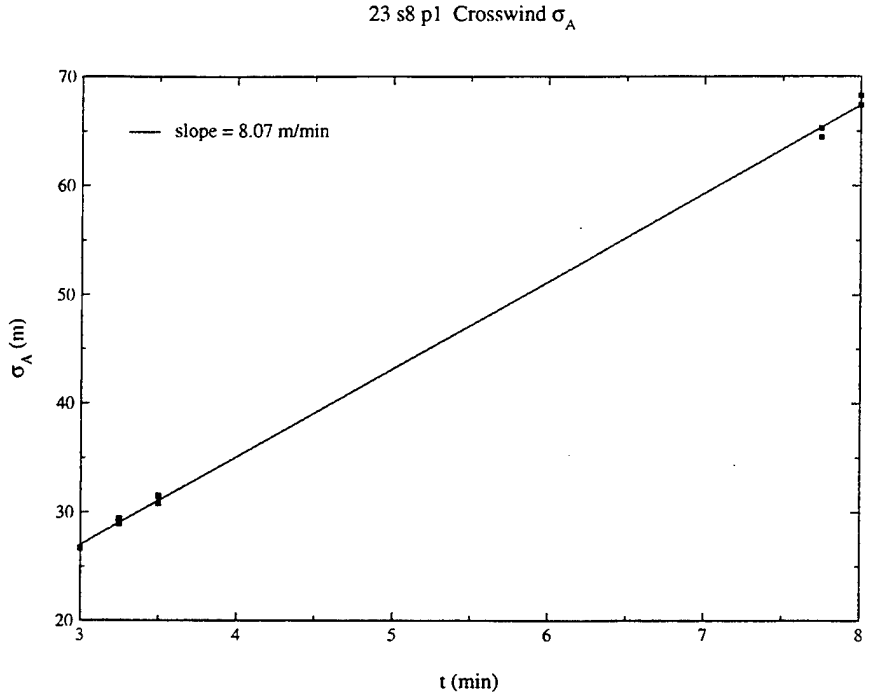

Figure 70: May 23 series 8 puff 1 Alongwind σ

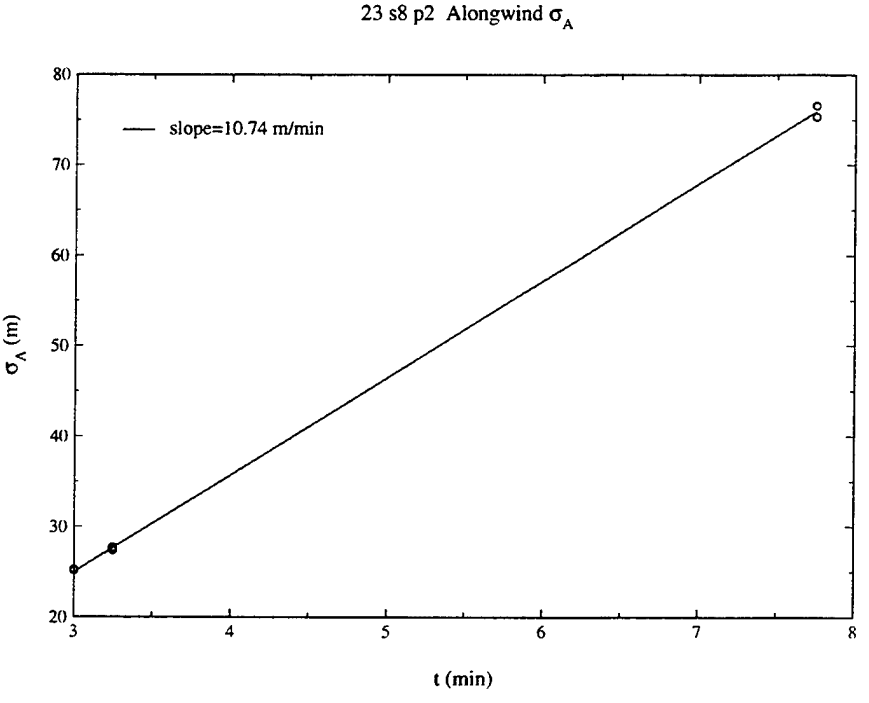

Figure 71: May 23 series 8 puff 2 Alongwind σ

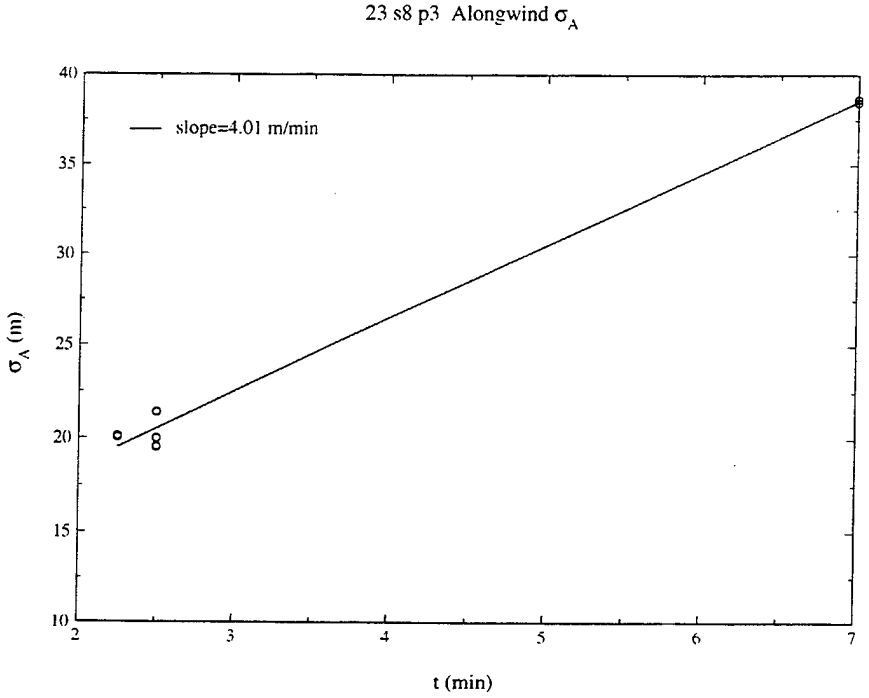

Figure 72: May 23 series 8 puff 3 Alongwind σ

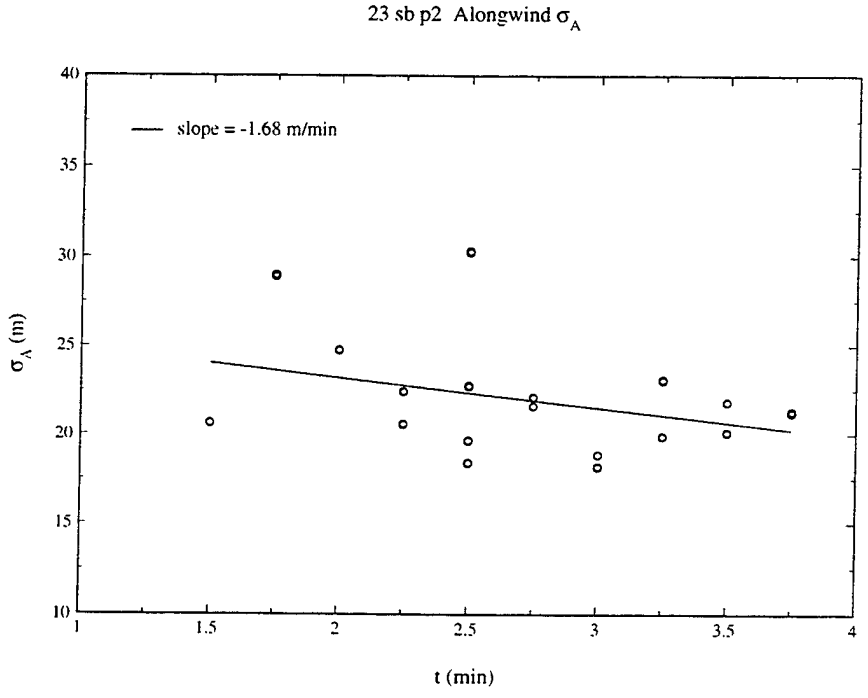

Figure 73: May 23 series b puff 2 Alongwind σ

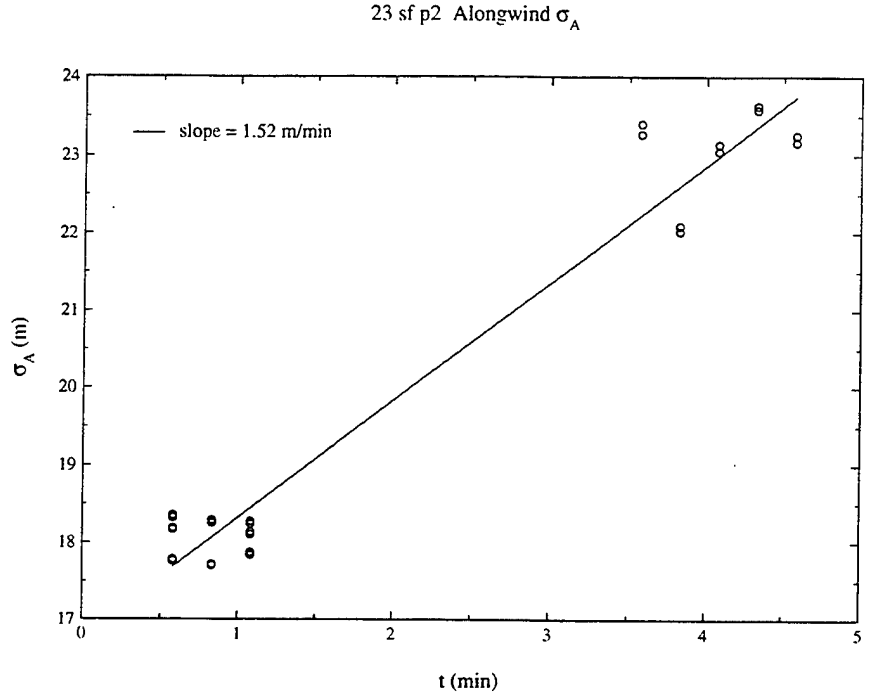

Figure 74: May 23 series f puff 2 Alongwind σ

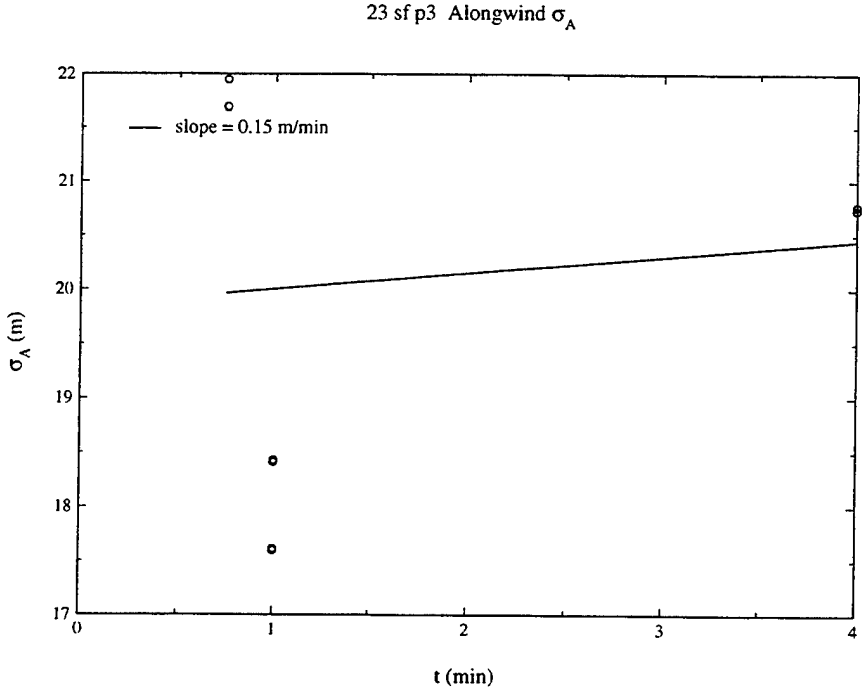

Figure 75: May 23 series f puff 3 Alongwind σ

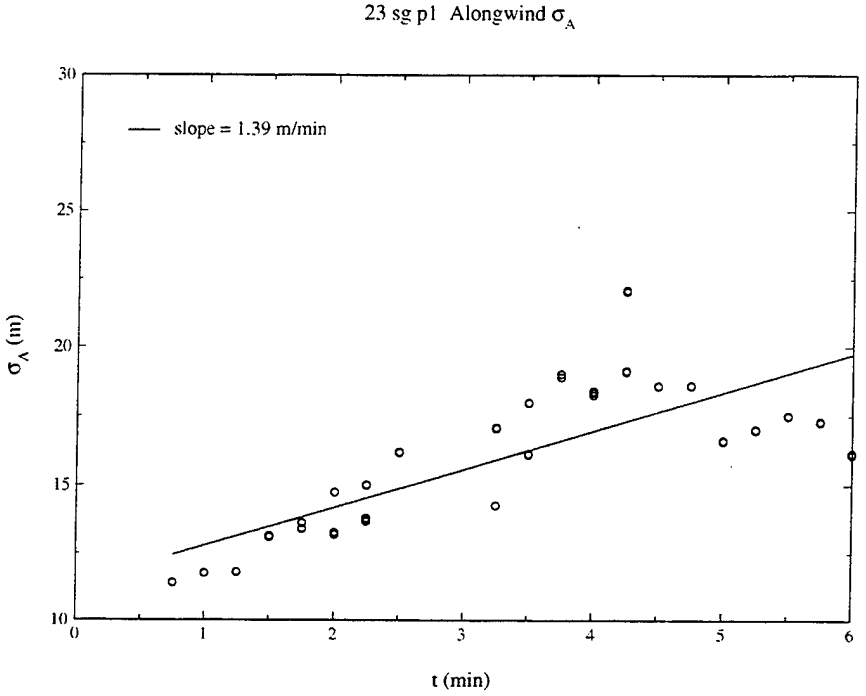

Figure 76: May 23 series g puff 1 Alongwind σ

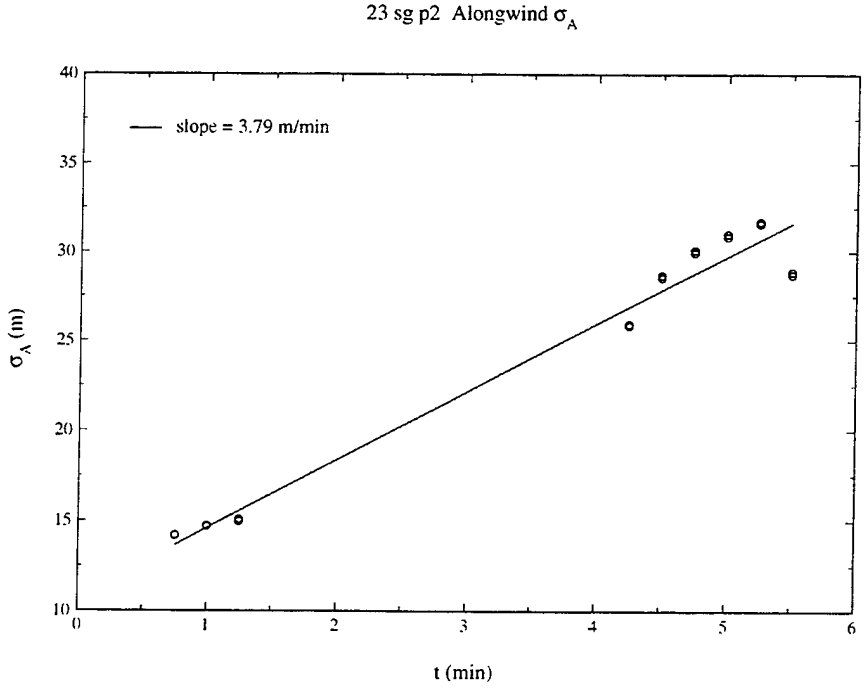

Figure 77: May 23 series g puff 2 Alongwind σ

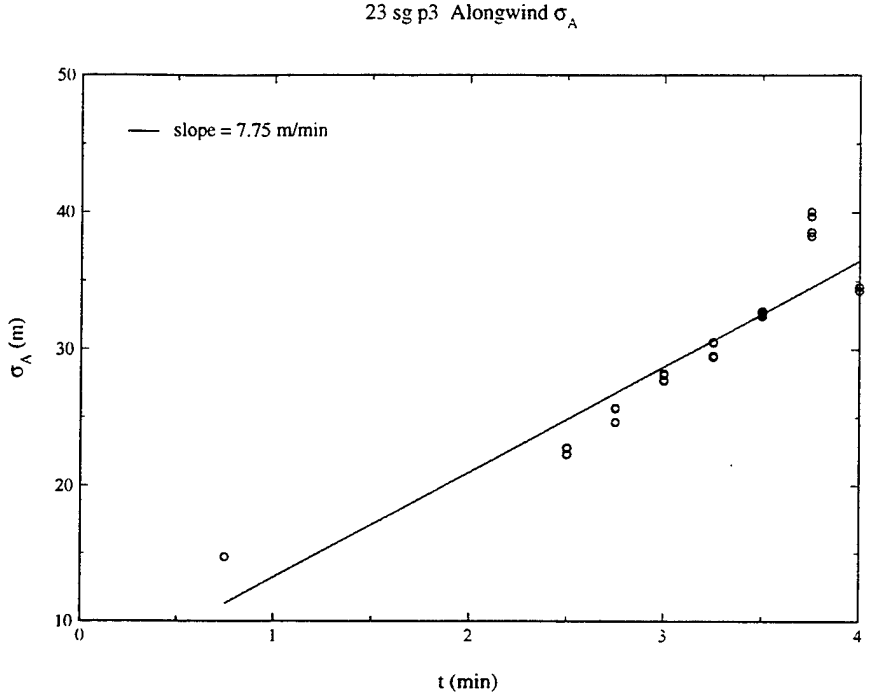

Figure 78: May 23 series g puff 3 Alongwind σ

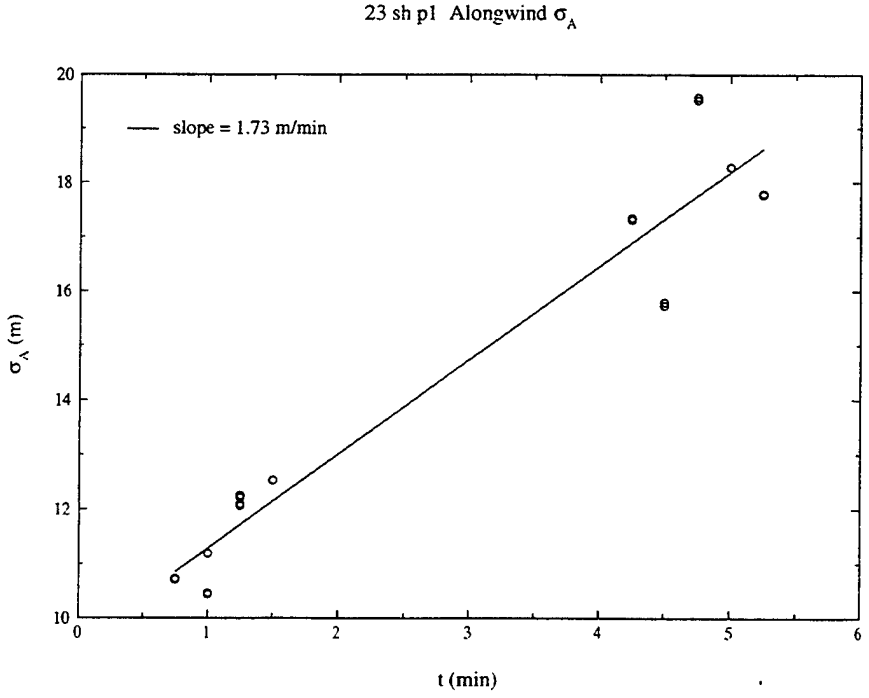

Figure 79: May 23 series h puff 1 Alongwind σ

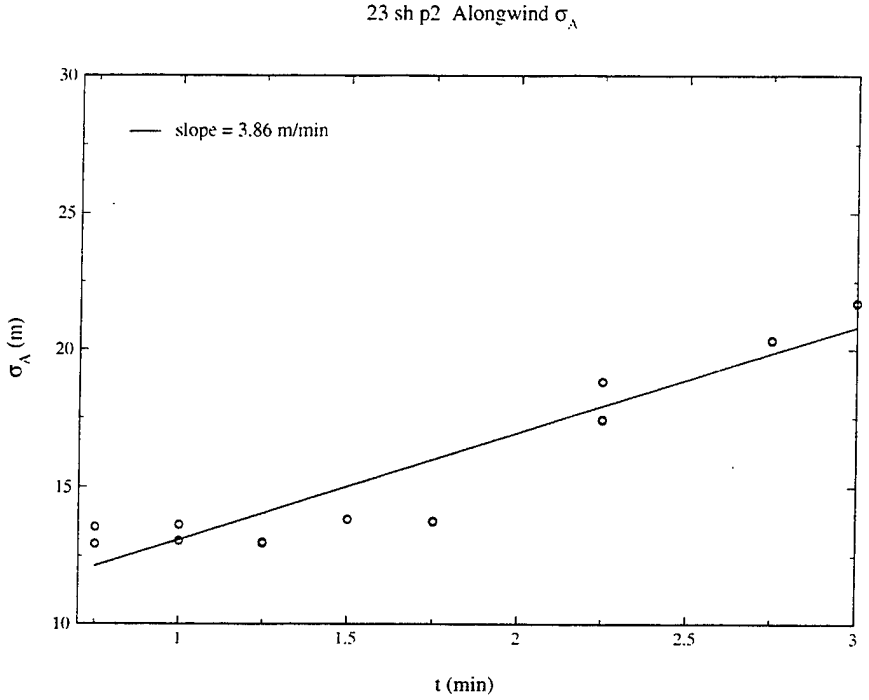

Figure 80: May 23 series h puff 2 Alongwind σ

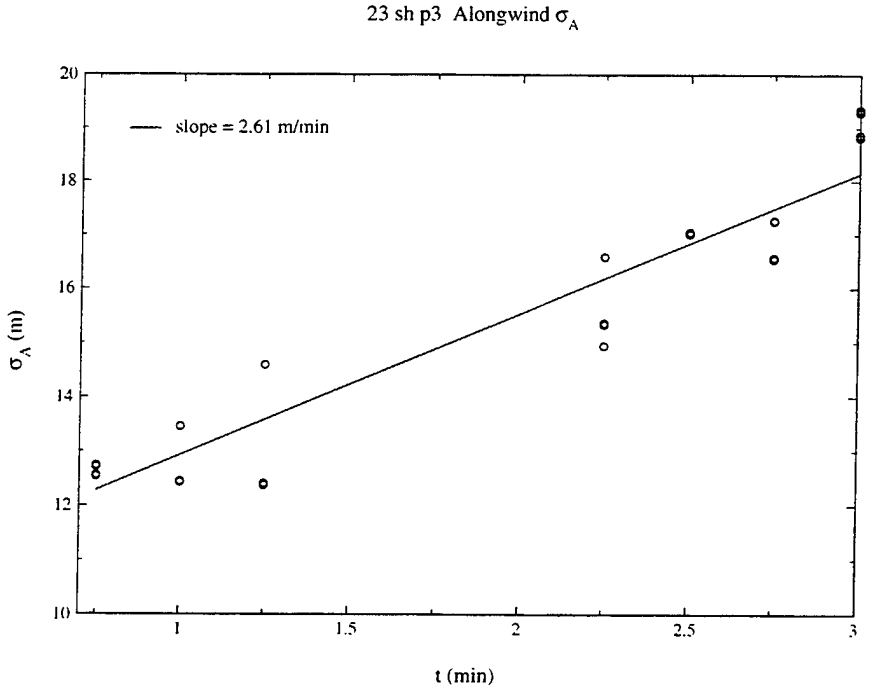

Figure 81: May 23 series h puff 3 Alongwind σ

Puff	Release Time (Z)	Puff Rt (m)	Puff thickness (m)	U (m/s)	Dir(deg) (from)	$d\sigma_{max}/dt$ (m/min)	i_{max} (βi=.44)	$d\sigma_{min}/dt$ (m/min)	i_{min} (βi=.44)
s1p1	21:00	785	240	3.85	322	2.5	0.037	11.4	0.169
s1p2	21:01	800	280	4.02	330	11.4	0.162	N/A	N/A
s2p1	21:15	841	280	5.00	324	9.0	0.103	3.1	0.036
s2p2	21:16	838	180	4.98	325	6.6	0.075	4.4	0.051
s2p3	21:17	834	180	5.00	321	9.7	0.110	4.5	0.051
s3p1	21:27	797	120	5.10	315	11.7	0.131	5.8	0.065
s3p2	21:28	800	95	5.02	313	4.0	0.045	2.9	0.033
s3p3	21:29	825	180	5.17	318	18.1	0.199	3.1	0.034
s4p1	21:38:30	820	240	5.50	320	20.6	0.213	5.2	0.053
s4p2	21:39:30	820	185	5.55	320	9.9	0.101	2.5	0.025
s4p3	21:40:30	820	180	5.50	317	14.8	0.152	2.8	0.029
s5p1	21:47	800	280	5.48	319	14.0	0.145	2.6	0.027
s5p2	21:48	780	170	5.57	315	21.3	0.217	5.1	0.052
s5p3	21:49	810	265	5.67	315	13.2	0.132	2.4	0.024

Figure 82: Summary of puff data from May 21

4 Data Summary

Summaries of puff data are shown in Figures 82 and 83 for May 21 and 23, respectively. The derivative $d\sigma/dt$ is used to estimate the turbulent intensity ($i = \sigma_u/U$ or $i = \sigma_v/U$), assuming the following linear relationship from Smith and Hay [11]

$$\frac{d\sigma}{dx} \approx \frac{2}{3}\beta i^2 \tag{3}$$

for puff expansion. Emperical evidence [8] suggests that βi is roughly constant with a value of 0.44 (assumed here). An assumed linear relationship between the turbulence value and the rate of puff σ growth is appropriate if the time period of interest ($\sim 500s$) of the puff growth is much less than the integral time scale (T_L) of the atmosphere above the boundary layer. The plots indicate that the linear growth can be assumed in many cases. In other cases it is clearly not appropriate over the entire regime under consideration. The data thus derived shows turbulence intensity i value of about 1 to 2 degrees for cases without persistent large scale shear. These issues and others, including comparision with meteorological data and application to REEDM algorithm evaluation, will be discussed in a subsequent report.

Puff	Release Time (Z)	Puff Ht (m)	Puff thickness (m)	U (m/s)	Dir (deg) (from)	$d\sigma_{cross}/dt$ (m/min)	i_{cross} (βi=.44)	$d\sigma_{along}/dt$ (m/min)	i_{along} (βi=.44)
S1P1	19:00	900	90	8.00	319	1.9	0.013	2.0	0.014
S1P2	19:01	890	90	7.92	320	2.9	0.021	1.6	0.012
S1P3	19:02	900		7.79	321	1.8	0.013	1.68	0.012
S2P1	19:10	900	80	7.59	320	4.6	0.035	3.82	0.029
S2P2	19:11	880	80	7.43	321	2.3	0.017	4.15	0.032
S2P3	19:12	900	100	7.47	318	1.7	0.013	5.79	0.044
S3P1	19:17	850	100	7.62	320	1.5	0.011	3.17	0.024
S3P2	19:18	900	100	7.82	317	2.6	0.019	N/A	N/A
S3P3	19:19	920	130	8.29	316	4.5	0.03[illegible]	N/A	N/A
S7P1	20:11	925	90	6.82	320	1.1	0.009	5.09	0.042
S7P2	20:11	925		6.74	320	1.4	0.012	3.88	0.033
S7P3	20:12	900	90	6.63	319	2.0	0.017	2.72	0.023
S8P1	20:18	925	75	7.16	320	4.0	0.032	8.07	0.064
S8P2	20:18	925	80	7.24	320	6	0.048	10.74	0.084
S8P3	20:19	925		7.45	318	7	0.057	4.01	0.031
SbP1	20:41	900	90	6.79	315	N/A	N/A	N/A	N/A
SbP2	20:42	920	130	6.81	316	N/A	N/A	-1.68	-0.014
SbP3	20:43	N/A		N/A	N/A	N/A	N/A	N/A	N/A
SfP1	21:38	885	80	6.45	315	0.1	0.001	N/A	N/A
SfP2	21:38	910	100	6.63	313	-0.5	-0.004	1.52	0.013
SfP3	21:39	920	105	6.58	314	0.2	0.002	0.15	0.001
SgP1	21:42	850	65	6.29	315	2.7	0.024	1.39	0.013
SgP2	21:42	830	100	5.95	312	1.9	0.018	3.79	0.036
SgP3	21:43	830	55	5.89	311	2.0	0.019	7.75	0.075
ShP1	21:45	830	70	6.42	314	3.6	0.032	1.73	0.015
ShP2	21:46	840		6.45	315	2.5	0.022	3.86	0.034
ShP3	21:46	850		6.59	315	2.4	0.020	2.61	0.023

Figure 83: Summary of puff data from May 23

References

[1] R. N. Abernathy, "MVP Deployment 4 (May 1977) – Tracer Gas Atmospheric Dispersion Measurements at Vandenberg Air Force Base," Aerospace Report TR-2000(1490)-2, 2000.

[2] R. N. Abernathy, personal communications.

[3] F. N. Frenkiel and I. Katz, "Studies of small-scale turbulence diffusion in the atmosphere," *J. Met.* **13**, 388, 1956.

[4] F. A. Gifford, "Relative atmospheric diffusion of smoke puffs," *J. Met.* **14**, 410, 1957.

[5] U. Högström, "An experimental study on atmospheric diffusion," *Tellus* **16**, 205, 1964.

[6] W. W. Kellogg, "Diffusion of smoke in the stratosphere," *J. Met.* **13**, 241, 1956.

[7] C. J. Nappo, "Turbulence and dispersion parameters derived from smoke-plume photoanalysis," *Atmospheric Environment* **18**, 299-306, 1984.

[8] F. Pasquill and F. B. Smith, *Atmospheric Diffusion*, Third Edition, 1983, Ellis Horwood Limited.

[9] M. Polak and J. T. Knudtson, personal correspondence.

[10] O. T. F. Roberts, "The theoretical scattering of smoke in a turbulent atmosphere," *Proc. Roy. Soc.* A **104**, 640, 1923.

[11] F. B. Smith and J. S. Hay, "The expansion of clusters of particles in the atmosphere," *Quart. J. R. Met. Soc.* **87**, 82-101, 1960.